MODELS OF ATMOSPHERIC WATER VAPOR BUDGET FOR THE TEXAS HIPLEX AREA

LP-117

TDWR CONTRACTS NO. 14-90026 AND NO. 14-00003

Prepared by:

DEPARTMENT OF METEOROLOGY
COLLEGE OF GEOSCIENCES
TEXAS A&M UNIVERSITY
COLLEGE STATION, TEXAS

Prepared for:

TEXAS DEPARTMENT OF WATER RESOURCES
AUSTIN, TEXAS

Funded by:

DEPARTMENT OF THE INTERIOR, WATER AND POWER RESOURCES SERVICE
TEXAS DEPARTMENT OF WATER RESOURCES

January 1980

MS-230 (8-70)
Bureau of Reclamation

TECHNICAL REPORT STANDARD TITLE PAGE

1. REPORT NO.	2. GOVERNMENT ACCESSION NO.	3. RECIPIENT'S CATALOG NO.

4. TITLE AND SUBTITLE
Models of the Atmospheric Water Vapor Budget for the Texas HIPLEX Area

5. REPORT DATE
December, 1979

6. PERFORMING ORGANIZATION CODE
580/330

7. AUTHOR(S)
Steven F. Williams and James R. Scoggins

8. PERFORMING ORGANIZATION REPORT NO.

9. PERFORMING ORGANIZATION NAME AND ADDRESS
Department of Meteorology
College of Geosciences
Texas A&M University
College Station, Texas 77843

10. WORK UNIT NO.
5540

11. CONTRACT OR GRANT NO.
14-06-D-7587

12. SPONSORING AGENCY NAME AND ADDRESS
Texas Department of Water Resources
P.O. Box 13087, Capitol Station
Austin, Texas 78711

Office of Atmospheric Resources Management*

13. TYPE OF REPORT AND PERIOD COVERED
Technical Report

14. SPONSORING AGENCY CODE

15. SUPPLEMENTARY NOTES
*Water and Power Resources Service
Denver Federal Center, Building 67
Denver, Colorado 80225

16. ABSTRACT
Water budget models were developed for the Texas HIPLEX area for convective and non-convective conditions, as a function of echo height, areal coverage, and type (isolated cells, clusters of cells, and lines of cells) of convective activity. Intra- and inter-comparisons of the water budget models indicate that greater amounts of water vapor are processed by increased depth and areal coverage of convective activity. Thus, the amount of convection seems to be more important than the type or presence of convective activity. An increased transport of water vapor near the surface is shown to be an important factor for increased convective activity. A "storage" of water vapor aloft was observed to correlate with cases of increased precipitation.

A comparison of all terms in the water budget equation indicates that the net horizontal transport of water vapor exceeds other terms in the equation as being the primary moisture source for all cases of convection. During periods of heavy precipitation, the net horizontal transport term nearly balanced the residual term, thus, making the net horizontal transport term the main source of water vapor for precipitation formation.

17. KEY WORDS AND DOCUMENT ANALYSIS

a. *DESCRIPTORS--* Water budget models, convective activity, moisture processes, mesoscale water vapor budgets, mesoscale systems, water vapor models, precipitation.

b. *IDENTIFIERS--* High Plains Cooperative Program (HIPLEX)
Big Spring-Snyder, Texas

c. *COSATI Field/Group*

18. DISTRIBUTION STATEMENT
Available from the National Technical Information Service, Operations Division, Springfield, Virginia 22151.

19. SECURITY CLASS (THIS REPORT)	21. NO. OF PAGES
UNCLASSIFIED	
20. SECURITY CLASS (THIS PAGE)	**22. PRICE**
UNCLASSIFIED	

MODELS OF THE ATMOSPHERIC WATER VAPOR BUDGET FOR THE TEXAS HIPLEX AREA

Steven F. Williams and James R. Scoggins
Department of Meteorology
College of Geosciences
Texas A&M University
College Station, Texas 77843

November 1979

Technical Report
TDWR Contract Nos. 14-90026 and 14-00003

Availability Unlimited

Prepared for
Texas Department of Water Resources
Austin, Texas

Funded by
Department of the Interior, Bureau of Reclamation, and the
State of Texas through the Texas Department of Water Resources

ACKNOWLEDGMENTS

The authors extend thanks to Drs. D. Djuric, A. B. Long, E. E. Gbur, and K. C. Brundidge, all of Texas A&M University, for reviewing the manuscript, Mr. John Rod for preparing the figures, and Mrs. Karen Hood for typing the manuscript.

This research was supported by the Bureau of Reclamation, Department of the Interior, and the Texas Department of Water Resources under TDWR Contract Nos. 14-90026 and 14-00003. This support is gratefully acknowledged.

EXECUTIVE SUMMARY

Mathematical models which approximate the quantity of moisture that passes through the atmosphere over the Texas HIPLEX area, called "water budget models," were developed for days in which thunderstorm activity occurs and for days in which this type of activity does not occur. These models were developed with respect to: (1) the vertical height of the clouds, (2) the area covered by the thunderstorm activity; and, (3) the physical characteristics of the thunderstorm activity, i.e., individual shower-producing clouds, clusters of shower-producing clouds, and lines of shower-producing clouds.

Inter- and intracomparisons of these water budget models indicate that greater amounts of moisture are processed when shower-producing cloud activity is deeper (grows taller into the atmosphere) and when a greater area is covered by the activity. This report suggests, then, that the amount of thunderstorm activity is more important than the physical characteristics of the shower-producing cloud activity in producing larger quantities of moisture.

Other related characteristics are revealed by this study. For example, an increased transport of moisture near the ground is shown to be an important factor for increased thunderstorm activity. Also, the presence of higher than normal amounts of moisture aloft (i.e. at heights of ten to eighteen thousand feet above the ground) correlates with the occurrence of precipitation.

The water vapor budget model is a complex mathematical equation with a number of terms representing the various physical and hydrodynamic effects of fluid motion. After evaluating statistically the relative importance of each of these terms, it is shown that a mathematical term which describes the net amount of moisture brought horizontally

into (or taken out of) a designated area over the Texas HIPLEX project area exceeds all other moisture-producing sources and, therefore is the primary source of moisture for shower-producing cloud development. During periods of heavy precipitation, this horizontal moisture flow term accounted for almost half of all moisture brought into the area of shower-producing cloud development. It is therefore concluded that this term represents the main source of moisture for precipitation formation over the Texas HIPLEX area.

TABLE OF CONTENTS

TABLE OF CONTENTS (Continued)

LIST OF FIGURES

LIST OF FIGURES (Continued)

LIST OF FIGURES (Continued)

LIST OF TABLES

LIST OF SYMBOLS AND UNITS USED

Symbol	Meaning	Units
A	Area of a vertical boundary	m^2
d	Distance between rawinsonde stations	m
i	Index representing 25 mb data	---
j	Index representing 50 mb data	---
k	Index representing horizontal sides of a volume	---
P	Pressure	mb
P_w	Precipitable water	g
q	Specific humidity or mixing ratio	$g\ g^{-1}$
r	Sources or sinks of water vapor per unit time	$g\ s^{-1}$
R	Residual term of the water vapor budget	$g\ s^{-1}$
R^*	Specific gas constant for dry air	$Nt\ m\ kg^{-1}{}^{\circ}K^{-1}$
s	Surface of a lateral boundary	---
s'	Surface of a volume	---
S	Sources or sinks of water vapor per unit time per unit volume	$g\ cm^{-3}\ s^{-1}$
t	Time	s
T	Temperature	deg Kelvin
T_L	Net transport of water vapor through lateral boundaries	$g\ s^{-1}$
T_V	Net transport of water vapor through vertical boundaries	$g\ s^{-1}$
v	Volume	m^3
V	Horizontal wind speed	$m\ s^{-1}$
V_n	Normal component of horizontal wind velocity	$m\ s^{-1}$
$\vec{V}_3$	Three dimensional wind vector	$m\ s^{-1}$
$(V_3)_n$	Normal component of three dimensional wind velocity	$m\ s^{-1}$
w	Kinematic vertical velocity	$m\ s^{-1}$
z	Height	gpm
ρ_a	Density of dry air	$kg\ m^{-3}$

Symbol	Meaning	Units
ϕ_1	Displacement angle between a triangular boundary and the normal axis	deg
ϕ_2	Horizontal wind direction	deg

1. INTRODUCTION

a. Statement of problem

Convective activity is one of the most important but insufficiently understood mesoscale phenomena today. This is primarily due to the vast amounts of water vapor and energy convective storms process on a small scale in both time and space. The environment therefore plays an important role in the transport and supply of water vapor essential for the growth and maintenance of convective activity. A basic knowledge of these interactions and interrelationships is essential before convective activity can be completely understood. An environmental water budget describes the transports, distributions, and supplies of water vapor associated with various forms of convective activity. Observations of differences in the water vapor budget for various types, depth, and areal coverage of convective activity should reveal important differences between such convective activity. Once this is achieved, the origin, existence, and the forecasting of convective clouds and their environment can be better understood.

b. Objectives

The objective of this research is to establish models of the water budget for the type, depth, and areal coverage of convective activity over the Texas HIPLEX (High Plains Experiment) area. This objective includes:

1) Description of environmental distributions and transports of water vapor accompanying convective activity;
2) Investigation of water vapor conversion to liquid water under various stages of convective activity;
3) Establishment of moisture sources and, therefore, latent energy sources for convective activity; and
4) Examination of factors leading to precipitation formation and determination of levels at which this occurs.

It is hoped that by achieving this objective, a better understanding of the interactions between convective activity and its environment will be achieved.

2. PREVIOUS STUDIES

Water budgets have been evaluated on the synoptic scale in an attempt to better understand convective systems (Braham, 1952; and Bradbury, 1957). Results showed only a fair agreement between observed and computed rainfall which indicates the need to examine station spacing in relation to convective activity. Because convective systems are of a small scale, the conventional upper air network is inadequate for studying processes relevant to a squall line or isolated thunderstorm (House, 1960). The need to study convective activity on a smaller scale was determined by Newton and Fankhauser (1964). The amount of water vapor intercepted by the storm is proportional to the diameter of the storm and its movement relative to the wind field. Thus, if the convective system is subsynoptic scale in size, pertinent individual effects from cloud-environment interactions will be missed. In fact, due to observational limitations in space and time, singular thunderstorm processes cannot be observed on a synoptic scale (Fankhauser, 1969).

Synoptic-scale budgets grossly underestimate moisture processes by smoothing out water vapor transport magnitudes in regions near convective activity. Greater rates of convergence and consumption of water vapor occur on a mesoscale (Fritsch, 1975). In the case for a tornado-producing squall line, the synoptic scale could only account for 10% of the mesoscale consumption rate of water vapor and only 20% of the rainfall rate. Substantial local circulations and water vapor transports on the mesoscale are apparently associated with organized convective lifting and compensating downdrafts (Fritsch *et al.*, 1976). Such water vapor transports would be missed in the evaluation of the water budget on a synoptic scale, and further demonstrate the need to evaluate the moisture source and, therefore, latent energy source of convective activity from a mesoscale approach.

Analysis of individual terms in the water budget was performed to find the relationship of the moisture source to convective activity. Palmen *et al.*, (1962) used a simplified water budget

equation to analyze an extra-tropical cyclone over the central United States. Results showed a strong dominance of horizontal convergence of water vapor which accounted for 95% of the observed rainfall. This study further indicated the importance of storm movement in relationship to the ambient wind field and available water vapor supplies (Newton and Fankhauser, 1964). In studies by Krishnamurti (1968) and Hudson (1971), large horizontal convergence of water vapor occurred in layers below cloud base. Strong correlations between low-level convergence of water vapor and the development of cumulus convection were found in observed cloud distributions. Foote and Fankhauser (1973) further studied low level convergence of water vapor by using aircraft measurements. They found that although convergence of water vapor occurred in all layers below cloud base, possibly only water vapor passing under the cloud at levels 3.0 km to cloud base actually entered the cloud. Fifty percent of this water vapor remained within the cloud in layers just above cloud base. The accumulation of water vapor near the surface by horizontal convergence prior to storm development is also an important factor in the development of convective activity (Lewis et al., 1974; and Fritsch, 1975).

Water vapor distributions have shown an accumulation of water vapor in ambient air aloft during the growth stages of a thunderstorm. Since this "storage" cannot be accounted for by convergence of water vapor in these layers, the thunderstorm acts as a pump to transport the water vapor aloft (Braham, 1952). This transport results in a drying below the level of water vapor storage except near the surface where cold moist air from the downdraft spreads out. Liquid water present in the cloud and a large fraction of the "storage" of water vapor is used to maintain the cold downdraft; and the resulting evaporation is largely responsible for a decrease in precipitation efficiency (Newton, 1966; and Foote and Fankhauser, 1973). Thus, for substantial precipitation amounts, a large supply of water vapor aloft is needed (Auer and Marwitz, 1968). Shallow non-precipitating clouds can in fact transport water vapor aloft to support neighboring deep precipitating clouds (Yanai et al., 1973). This is especially true for a squall line in which there is an interaction between

neighboring thunderstorms. McNab and Betts (1978) further studied the storage of water vapor in clouds prior to convection by the use of a "cloud storage" model as an integral part of their water budget. Their results demonstrated the importance of water vapor storage and at times this storage exceeded other source terms in developing convective activity leading to precipitation formation.

Previous studies described above have indicated the importance of the environment in the development and maintenance of convective activity. However, it is not clear how the environment responds to the type, depth, and amount of convective activity. Mesoscale models of the water budget should indicate differences in response and clarify the interaction between convective activity and its environment.

3. DATA UTILIZED

a. Rawinsonde

The data used in this study consist of upper air soundings taken at three rawinsonde stations (Midland, Post, and Robert Lee) in the Texas HIPLEX area on nine days during the summer of 1976, and on sixteen days during the summer of 1977. These soundings were taken at 3-h intervals from 1500 to 0300 GMT with an additional launch at 0600 GMT on some days during the summer of 1977. The sounding data consist of thermodynamic and wind data at 25-mb intervals interpolated from pressure contact and 30-sec wind data using the method described by Fuelberg (1974).

b. Precipitation

Precipitation data over the Texas HIPLEX area were provided by the Bureau of Reclamation for two days during the summer of 1976. The data consist of isohyetal charts of rainfall integrated to give total hourly volumes in acre-feet.

c. Radar

Hourly WSR-57 radar data were obtained from the National Weather Service at Midland, Texas. These data consisted of plan position indicator (PPI) traces of echoes over the Texas HIPLEX area. These data were manually digitized on a grid of 15.8 km and computer plotted. The categories digitized at each grid point were: no echoes, echo tops less than 6.1 km, echo tops between 6.1 and 9.1 km, and echo tops exceeding 9.1 km. Radar data used corresponded to the upper air sounding times described above in Section 3a.

4. DERIVATION OF THE WATER BUDGET EQUATION

The equation for conservation of water substance has been derived by Haltiner (1971) and may be expressed in the form:

$$\frac{\partial(\rho_a q)}{\partial t} + \vec{\nabla}_3 \cdot (\rho_a q \vec{V}_3) + S = 0 \tag{1}$$

where ρ_a is the density of dry air, q is the specific humidity, $\vec{V}_3$ is the three-dimensional wind vector, and S represents sources and sinks of water vapor in mass per unit volume per unit time. Applying Gauss's divergence theorem to Eq. (1) and integrating over volume yields:

$$\int_v \frac{\partial(\rho_a q)}{\partial t} dv + \int_{s'} (\rho_a q (V_3)_n) ds' + \int_v S dv = 0 \tag{2}$$

where $(V_3)_n$ represents the normal wind components to the boundaries of the volume, and s' represents the surface of the volume. Equation (2) can be expanded to include horizontal and vertical components of water vapor transport:

$$\int_v \frac{\partial(\rho_a q)}{\partial t} dv + \int_s (\rho_a q V_n) ds + \int_A (\rho_a q w) dA + r = 0 \tag{3}$$

where V_n is the normal wind component to the lateral boundaries of the volume, w is the normal wind component to the horizontal boundaries of the volume, A represents the horizontal surfaces of the volume, s represents the lateral surfaces of the volume, and r represents sources and sinks of water vapor per unit time for the volume. By assuming an incompressible and homogeneous atmosphere (ρ_a = constant) and using perturbation theory, Eq. (3) becomes:

$$\int_v (\rho_a \frac{\partial \bar{q}}{\partial t}) dv + \int_s (\rho_a \bar{q}\, \overline{V_n}) ds + \int_s (\rho_a \overline{q' V_n'}) ds + \int_A (\rho_a \bar{\bar{q}} \bar{\bar{w}}) dA +$$

$$\int_A (\rho_a \overline{q' w'}) dA + r = 0 \tag{4}$$

where barred quantities refer to mean values and prime quantities to fluctuation or perturbation quantities. Equation (4) can be simplified by grouping sources and sinks of water vapor with terms containing perturbation quantities and expressed as:

$$\int_V (\rho_a \frac{\partial \bar{q}}{\partial t}) dv + \int_S (\rho_a \bar{q} \overline{V_n}) ds + \int_A (\rho_a \overline{\bar{q}\bar{w}}) dA + R = 0 \qquad (5)$$

(1) (2) (3) (4)

where R represents the residual term of the water budget. Equation (5) represents the water budget at any particular time expressed as mass per unit time. The terms in the equation have the following interpretation: (1) the local rate-of-change or the net gain or loss of water vapor within the volume; (2) transport of water vapor through lateral boundaries; (3) transport of water vapor through horizontal boundaries; and (4) the sources and sinks of water vapor (evaporation, condensation and some of which eventually may be lost through precipitation, and the turbulent flux of water vapor or translation of cloud liquid water through the boundaries). Because of the sign convention used with V_n and w in the calculations, terms (2) and (3) will be positive when there is a net gain of water vapor and negative for a net loss of water vapor in the volume.

5. METHODS OF COMPUTATION OF TERMS IN THE WATER BUDGET EQUATION

The Texas HIPLEX area spans nearly 43,000 km^2 and is centered approximately at Big Spring, Texas. A triangular area within the Texas HIPLEX area was formed by the vertices of three rawinsonde stations as shown in Fig. 1. The effect of balloon drift at this

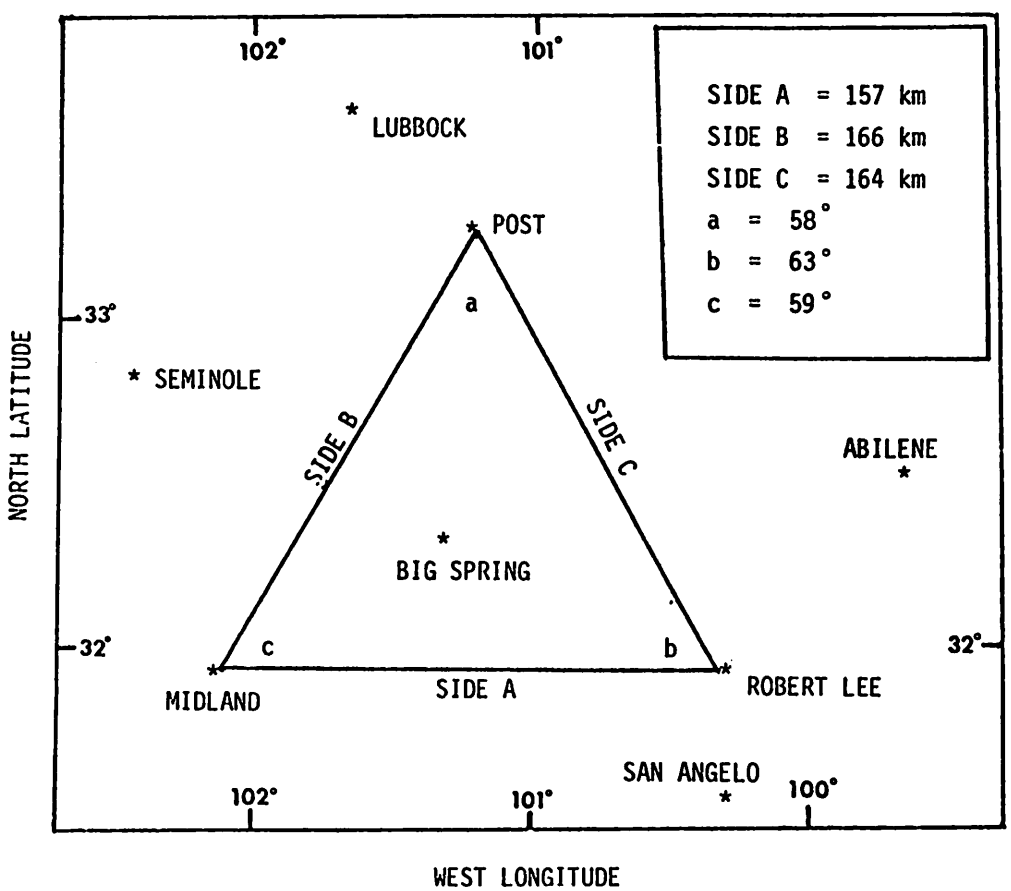

Fig. 1. Triangle for which water budget is determined.

scale is assumed to be negligible for summertime winds so this triangular area remains essentially constant with height. Equation (5) is evaluated for the volume defined by this area multiplied by the vertical distance between 50-mb levels from 850 to 300 mb. No transport of water vapor is assumed above 300 mb due to the small water vapor amounts there.

A sample 50-mb layer over the Texas HIPLEX area is shown in Fig. 2.

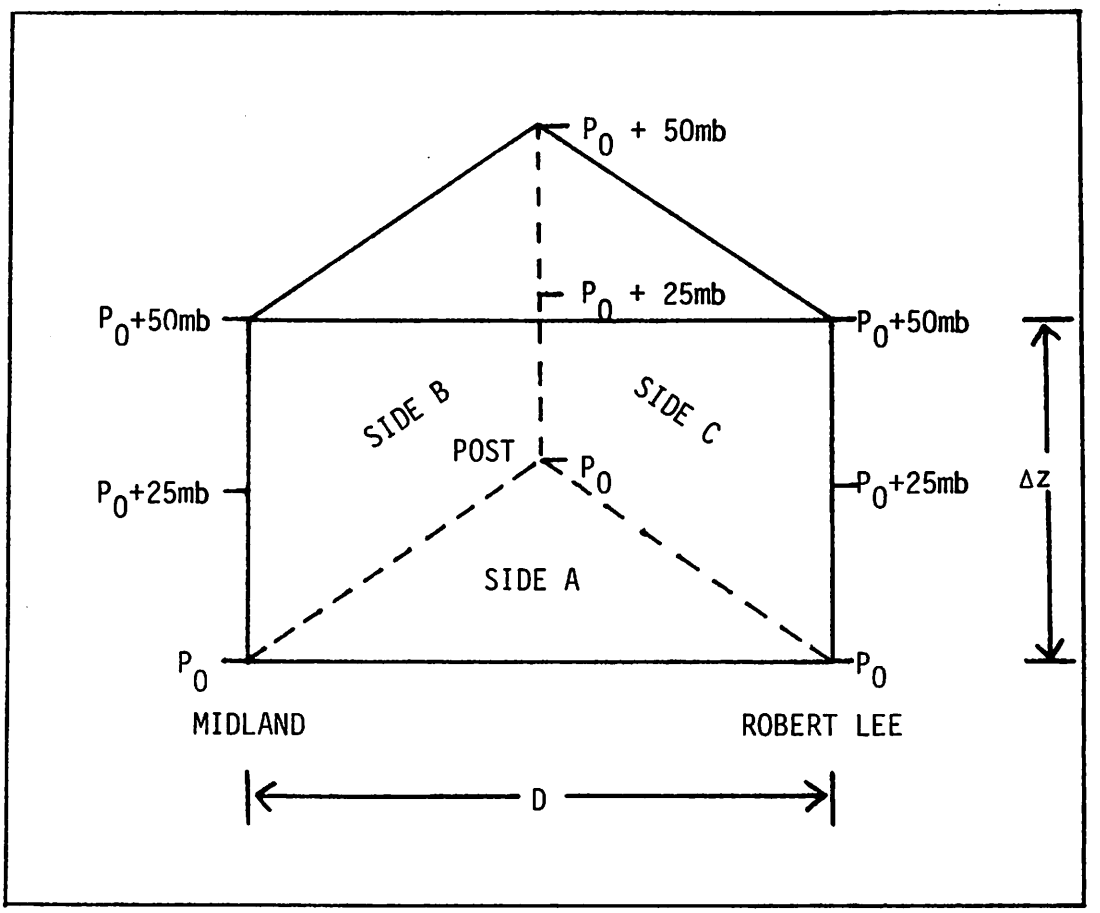

Fig. 2. Example of volume 50-mb deep used to evaluate terms in the water budget.

Data points at 25-mb intervals for each station are also denoted for use below in describing methods of computation for the water budget terms.

a. Local rate-of-change in water vapor

Haltiner and Martin (1957) define the precipitable water in a column of air as the total mass of water vapor per unit area in the column. Here, we shall define precipitable water as:

$$P_w = \int_z \int_A (q\ \rho_a) dA\ dz \qquad (6)$$

where z represents the height, A represents the area and q represents the specific humidity which may be approximated by the mixing ratio

(Haltiner, 1971) (q will be retained for the symbol for mixing ratio). Integrating Eq. (6) over a 50-mb volume yields:

$$P_w = (\overline{q\rho_a})A\,\overline{\Delta z} \tag{7}$$

where $\overline{q\rho_a}$ is the mean density of water vapor within the volume, A is the triangular area, and $\overline{\Delta z}$ is the mean depth of the 50-mb layer. By using 25-mb data as shown in Fig. 2, mean quantities of water vapor density and height can be computed according to the following approximations:

$$\overline{q\rho_a} = \frac{1}{9}\left(\sum_{i=1}^{9} (R^*)^{-1}\,\frac{q_i P_i}{T_i}\right) \tag{8}$$

and

$$\overline{\Delta z} = \frac{1}{3}\left(\sum_{j=1}^{3} (\Delta z)_j\right) \tag{9}$$

where R* represents the specific gas constant for dry air, P is the pressure, T is the temperature, Δz represents the height between 50-mb levels for each station determined from the hypsometric equation, i represents 25-mb data, and j represents 50-mb data. By substituting Eqs. (8) and (9) into Eq. (7) yields a new expression for the total mass of water vapor for the volume at a given time:

$$P_w = \frac{A}{27}\left(\sum_{i=1}^{9} (R^*)^{-1}\,\frac{q_i P_i}{T_i}\right)\left(\sum_{j=1}^{3} (\Delta z)_j\right). \tag{10}$$

To determine the local rate-of-change of the total mass of water vapor for each layer, various time differencing schemes are applied to Eq. (10). For the first and final sounding time each day, a 3-h forward and backward time difference scheme is applied, respectively. For all other times a 6-h centered time difference is used.

b. Net transport of water vapor through lateral boundaries

Term (2) of Eq. (5) is integrated over a 50-mb layer which yields:

$$T_L = \sum_{k=1}^{3} (\overline{q\rho_a V_n})_k (\overline{\Delta z})_k d_k \tag{11}$$

where T_L represents the net transport of water vapor through lateral boundaries, k represents a side of the triangle shown in Fig. 1, d represents the distance between rawinsonde stations, $\overline{\Delta z}$ represents the mean depth of a 50-mb layer computed from the hypsometric equation, and the bars represent spatial averages.

By considering only one side of the triangle and using 25-mb data as shown in Fig. 2, the mean value of transport of water vapor density and the mean depth of a 50-mb layer can be expressed in finite form:

$$\overline{q\rho_a V_n} = \frac{1}{6}\left(\sum_{i=1}^{6} (R^*)^{-1} \frac{q_i P_i}{T_i} (V_n)_i\right) \tag{12}$$

and

$$\overline{\Delta z} = \frac{1}{2}\left(\sum_{j=1}^{2} (\Delta z)_j\right). \tag{13}$$

By substituting Eqs. (12) and (13) into Eq. (11) for one lateral boundary gives the following expression:

$$(T_L)_k = \frac{d_k}{12}\left(\sum_{i=1}^{6} (R^*)^{-1} \frac{q_i P_i}{T_i} (V_n)_i\right)_k \left(\sum_{j=1}^{2} (\Delta z)_j\right)_k. \tag{14}$$

The component of horizontal wind velocity normal to a boundary is determined by the expression:

$$V_n = V \sin(\phi_1 - \phi_2) \tag{15}$$

where V is the scalar wind speed, ϕ_2 is the direction from which the wind is blowing, and ϕ_1 is the displacement angle between the boundary and the N-S axis measured clockwise from north. Each displacement angle is a function of the orientation of individual boundaries to true north. By evaluating Eq. (15) for each boundary at each data point shown in Fig. 2 yields:

$$\text{SIDE A} \quad (V_n)_i = [V \sin(273 - \phi_2)]_i, \tag{16}$$

$$\text{SIDE B} \quad (V_n)_i = [V \sin(27 - \phi_2)]_i, \tag{17}$$

and

$$\text{SIDE C} \quad (V_n)_i = [V \sin(155 - \phi_2)]_i \tag{18}$$

where a positive $(V_n)_i$ represents a flow into the volume.

The transport of water vapor through each lateral boundary shown in Fig. 1 can be computed by substituting Eqs. (16) - (18), respectively, into Eq. (14). The net transport of water vapor into the volume through lateral boundaries or the net horizontal transport of water vapor is determined by the algebraic sum of Eq. (14) for all three boundaries. This net total represents the transport of water vapor into the volume minus the transport of water vapor out of the volume through the lateral boundaries.

c. Transport of water vapor through horizontal boundaries

Term (3) in Eq. (5) can be integrated over the area shown in Fig. 1. The vertical transport of water vapor through one horizontal boundary can be expressed as:

$$(T_v)_j = (\overline{q\rho_a}\ \bar{w})_j A \tag{19}$$

where A represents the triangular area shown in Fig. 1, and $\bar{w}$ represents the "kinematic" vertical velocity obtained by integration of the continuity equation in pressure coordinates from the surface upwards in 50-mb intervals (Wilson, 1976). A conversion from pressure coordinates was applied utilizing the hydrostatic approximation. Mean values of the density of water vapor also were computed every 50 mb using 50-mb data shown in Fig. 2. The product of these quantities is given by:

$$\overline{q\rho_a}\ \bar{w} = \frac{1}{3}\left(\sum_{j=1}^{3} (R^*)^{-1} \frac{q_j P_j}{T_j}\ \bar{w}\right). \tag{20}$$

Substitution of Eq. (20) into Eq. (19) yields:

$$(T_v)_j = \frac{A}{3}\left(\sum_{j=1}^{3} (R^*)^{-1} \frac{q_j P_j}{T_j}\ \bar{w}\right) \tag{21}$$

which represents the vertical transport of water vapor through constant pressure surfaces, and its sign is a function of the vertical velocity.

d. The net transport of water vapor through horizontal boundaries

The net transport of water vapor in a 50-mb layer through horizontal boundaries represented by term (3) in Eq. (5) can be computed for each

layer as the difference between the transports of water vapor through the top and bottom boundaries of that layer. The result is expressed mathematically as:

$$T_v = \frac{A}{3}\left[\left(\sum_{j=1}^{3} (R^*)^{-1} \frac{q_j P_j}{T_j} \bar{w}_j\right) - \left(\sum_{j+1=1}^{3} (R^*)^{-1} \frac{q_{j+1} P_{j+1}}{T_{j+1}} \bar{w}_{j+1}\right)\right]. \qquad (22)$$

This value represents the transport of water vapor into the volume minus the transport of water vapor out of the volume through vertical boundaries.

e. Combined net transport of water vapor through lateral and horizontal boundaries

The combined net transport of water vapor through lateral and horizontal boundaries is computed as the algebraic sum of the net transport of water vapor through lateral boundaries and the net transport of water vapor through horizontal boundaries. This is the algebraic sum of terms (2) and (3) in Eq. (5). This value represents the total net transport of water vapor entering the volume minus the transport of water vapor leaving the volume, through all the boundaries of a 50-mb layer.

f. The residual term of the water budget

The residual term of the water budget may include precipitation, evaporation, condensation, or the turbulent flux of water vapor through lateral and vertical boundaries or a combination of these. It represents the negative of the algebraic sum of terms (1), (2), and (3) in Eq. (5), since this equation was derived under the assumption of continuity of water substance. In the interpretation of the residual term, precipitation and condensation represent a sink or loss of water vapor, evaporation represents a source or gain of water vapor, and the turbulent flux of water vapor through lateral and horizontal boundaries can represent a source or sink of water vapor. No attempt to distinguish individual components comprising the residual term will be undertaken here, but it will be discussed in a later section.

6. STRATIFICATION OF COMPUTED RESULTS FOR EACH SOUNDING TIME

The terms in Eq. (5) were evaluated in each 50-mb layer from 850 to 300 mb for every sounding time for which data from all three rawinsonde stations in Fig. 1 were available. The computed results were stratified according to the presence, type, depth, and areal coverage of echoes using the digitized radar data.

The results were first stratified into two major groups: (1) sounding times when no echoes were observed over the triangular area; and (2) sounding times when echoes were observed over the triangular area. This stratification was independent of the type, depth, and areal coverage of echoes. Each term in the water budget was averaged for each 50-mb layer and average vertical profiles constructed for each group.

For all times when convective activity was observed over the triangular area, results were stratified according to the type of echo observed: (1) sounding times when isolated convective cells were observed; (2) sounding times when clusters of convective cells were observed; and (3) sounding times when a distinct line of convective cells were observed. This stratification was completely independent of depth and areal coverage of echoes. Each term in the water budget was averaged for each 50-mb layer and average vertical profiles constructed for each group.

For all times that convective activity was present over the triangular area, the results were stratified according to the depth or "intensity" of echoes: (1) sounding times when tops less than 6.1 km were observed; (2) sounding times when tops between 6.1 and 9.1 km were observed; and (3) sounding times when tops greater than 9.1 km were observed. The data were stratified according to the highest top observed over the triangular area if more than one of the stratification conditions was satisfied. This stratification was independent of the type and areal coverage of the echoes. Each term in the water budget equation was averaged for each 50-mb layer and average vertical profiles constructed for each group.

For all sounding times when convective activity was observed over the triangular area, results were stratified according to the areal coverage of the echoes: (1) sounding times when echoes covered 50% or more of the area; and (2) sounding times when echoes covered less than 50% of the area. This stratification was independent of the type or depth of echoes. Each term in the water budget was averaged for each 50-mb layer and average vertical profiles constructed for each group.

The total number and percent of soundings in each stratification are shown in Table 1. When convective echoes were observed over the triangular area, the highest percentage of soundings stratified consist of clusters of cells, cells with tops less than 6.1 km, and areal coverage less than 50%.

Table 1. Stratification of data for all sounding times.[1]

ECHOES	STRATIFICATION	NUMBER OF CASES IN EACH CATEGORY	PERCENT OF CASES IN EACH CATEGORY
Presence	Non-convective	66	58
	Convective	48	42
Type	Cluster of cells	19	40
	Lines of cells	15	31
	Isolated cells	14	29
Depth	Tops less than 6.1 km	23	48
	Tops greater than 9.1 km	13	27
	Tops between 6.1 and 9.1 km	12	25
Areal Coverage	Less than 50% areal coverage	26	54
	Greater than or equal to 50% areal coverage	22	46

[1] 114 total sounding times obtained from the data.

7. MODELS OF THE WATER BUDGET

Models for the water budget have been constructed from the presence, type, depth, and areal coverage of convective activity. Each of these models include average vertical profiles of the net horizontal transport of water vapor, net vertical transport of water vapor, vertical transport of water vapor through constant pressure surfaces, combined net horizontal and vertical transport of water vapor, local rate-of-change in the total mass of water vapor, and the residual term for several stratifications. Due to the small sample size standard deviations of the average profiles are not presented. Each model descriptively analyzes similarities and differences observed between stratification criteria. Intra- and inter-comparisons of the models are made. For purposes of describing water vapor transports in relation to convective activity, an average cloud base observed over the Texas HIPLEX area between 700 and 750 mb is used. The average surface pressure for the Texas HIPLEX area was observed to be approximately 920 mb.

a. Convective and non-convective

Figures 3-8 represent vertical profiles for convective and non-convective models of the water budget. For convective cases, a net gain in the horizontal transport of water vapor (Fig. 3) is observed in all layers with the largest gain near the surface and at approximately 600 mb. This strong convergence indicates the importance of water vapor aloft needed for deep convective growth and development. Conversely, for cases of nonconvection, a net loss of water vapor occurs above 600 mb, although a net gain is observed below 600 mb. These results agree with those of McNab and Betts (1978) for cases of weak convection. The subcloud convergence of water vapor is indicative of "fair weather" cumulus formation which does not develop deeply due to the lack of water vapor aloft. Although horizontal convergence of water vapor below 650 mb occurs in all cases, the magnitudes are larger for cases of convection. This further indicates the importance of subcloud horizontal convergence of water vapor in sustaining deeper convection.

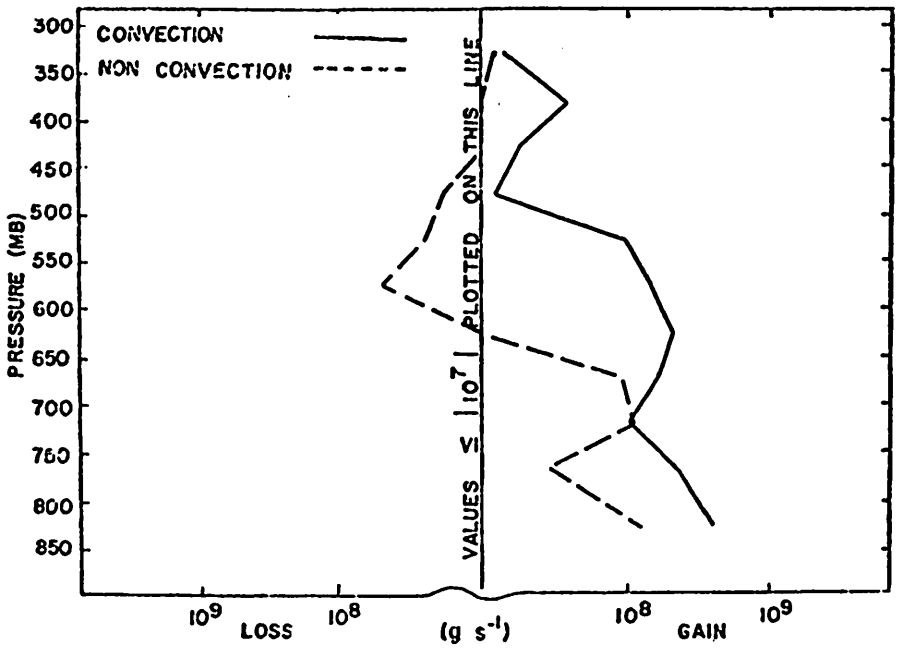

Fig. 3. Net horizontal transport of water vapor through boundaries of 50-mb layers (g s^{-1}) over the Texas HIPLEX area for average convective and non-convective cases.

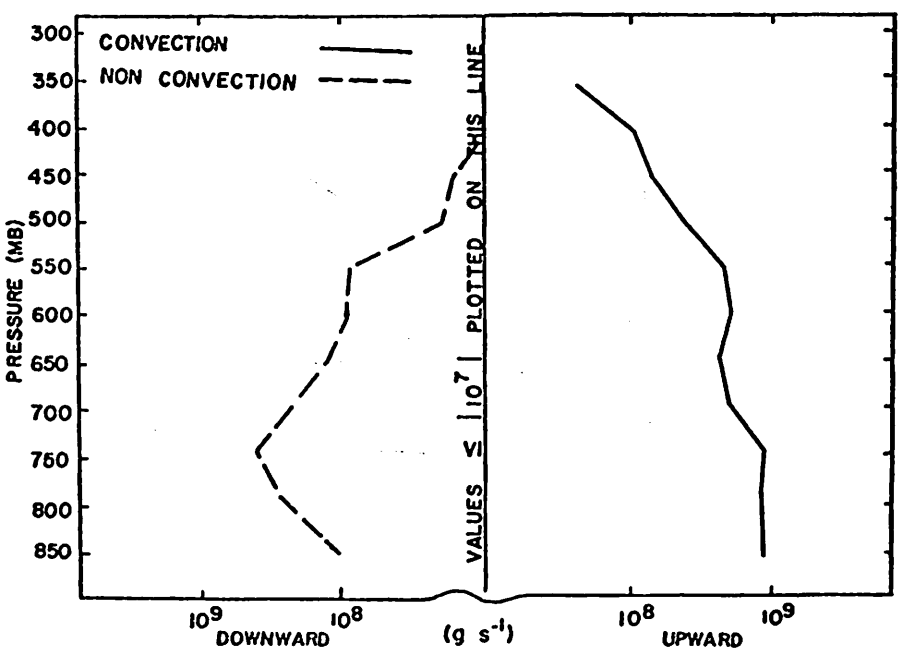

Fig. 4. Vertical transport of water vapor through constant pressure surfaces (g s^{-1}) over the Texas HIPLEX area for average convective and non-convective cases.

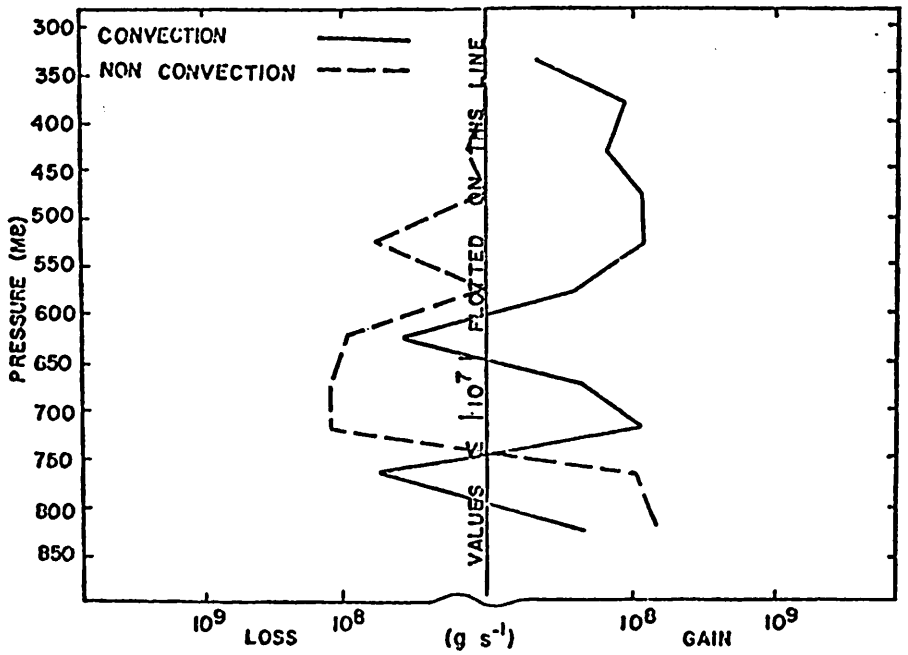

Fig. 5. Net vertical transport of water vapor through boundaries of 50-mb layers (g s^{-1}) over the Texas HIPLEX area for average convective and non-convective cases.

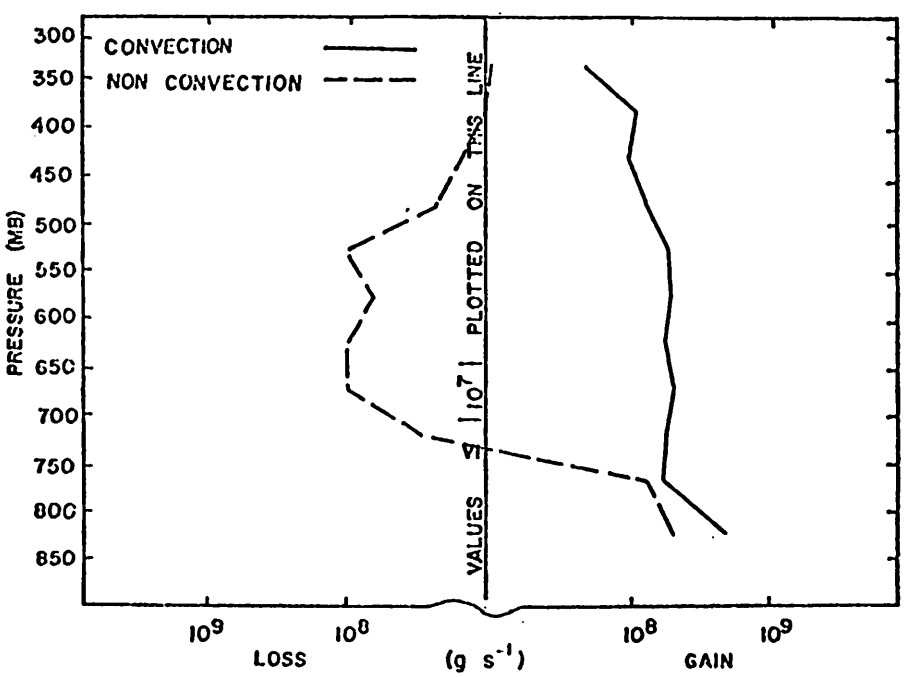

Fig. 6. Combined net horizontal and vertical transport of water vapor through boundaries of 50-mb layers (g s^{-1}) over the Texas HIPLEX area for average convective and non-convective cases.

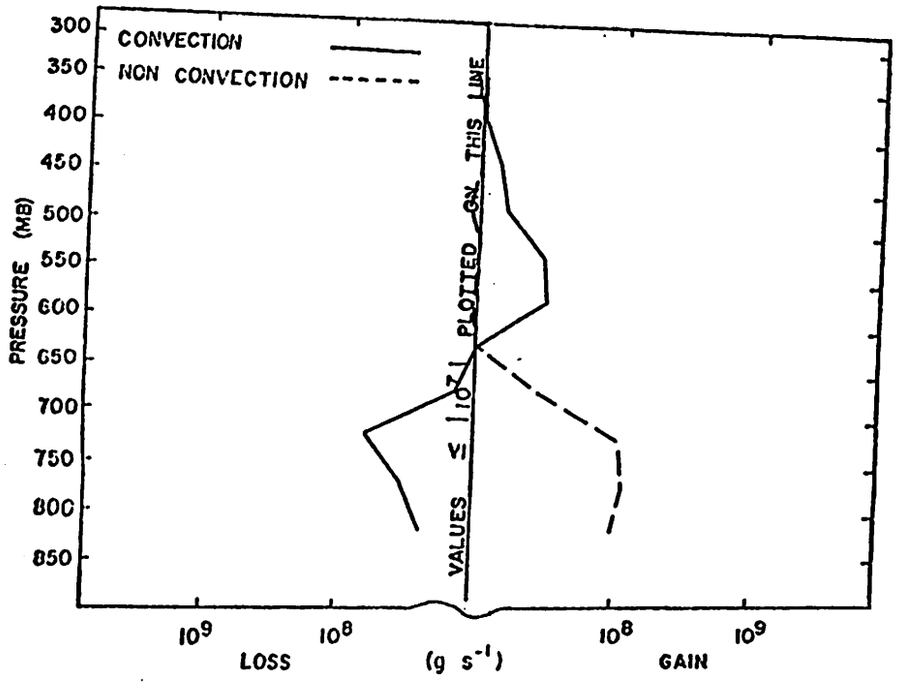

Fig. 7. Local rate-of-change in the total mass of water vapor (g s^{-1}) over the Texas HIPLEX area for average convective and non-convective cases.

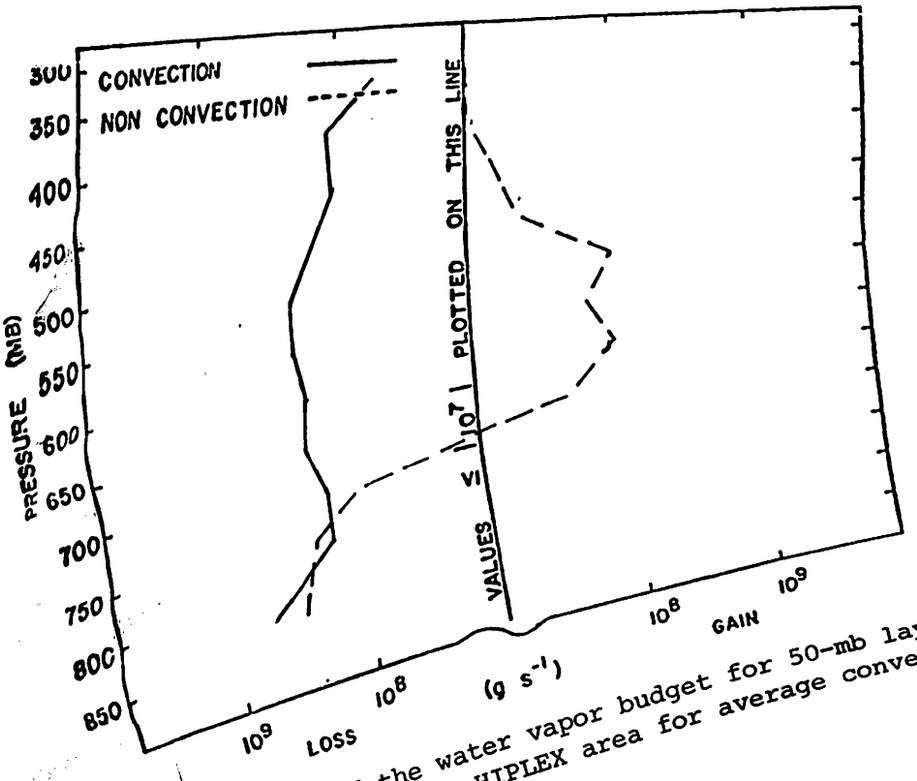

Fig. 8. Residual term of the water vapor budget for 50-mb layers in (g s^{-1}) over the Texas HIPLEX area for average convective and non-convective cases.

b. Isolated, clusters, and lines of convective cells

Large differences in water vapor processes exist between several classifications of convective activity shown in Figs. 9-14. The net horizontal transport of water vapor (Fig. 9) shows a large inflow at all layers for clusters of cells. This profile basically resembles that for all cases of convection which shows a large net gain in water vapor both near the surface and at 600 mb. The profile for lines of cells also shows a large net gain both near the surface and between 650 mb and 500 mb. The profile for cases of isolated cells shows a net loss near 750 mb and 500 mb. A comparison of profiles for various types of convective activity indicates large changes with height in the net horizontal transport of water vapor especially for isolated cells. However, the size and number of these cells could introduce variation in determining the profile for isolated cell cases. A similar net horizontal gain in water vapor occurs at approximately 650 mb for all cases which indicates a water vapor source which is independent of the type of convection involved.

The vertical transport of water vapor through constant pressure surfaces (Fig. 10) shows strong upward transport for clusters and lines of cells. In fact lines of cells exhibit a slightly larger upward transport at all levels than clusters of cells. This might be attributed to an interaction and organized lifting between cells within the line. Yanai et al., (1973) determined that shallower non-precipitating clouds transfer water vapor aloft to support neighboring precipitating ones. The profile for cases of isolated cells again shows large variation with height, with weaker water vapor transports than cases of clusters and lines of cells.

Profiles of net vertical transport of water vapor (Fig. 11) show greater variation than the net horizontal transport. The profile for lines of cells still shows the greatest net gain especially at 700 mb and above 500 mb. The same is true for clusters of cells, but to a lesser magnitude. For cases of isolated cells, a larger net gain is observed near the surface with divergence aloft below 550 mb which is similar to the profile for nonconvective cases (Fig. 5). The

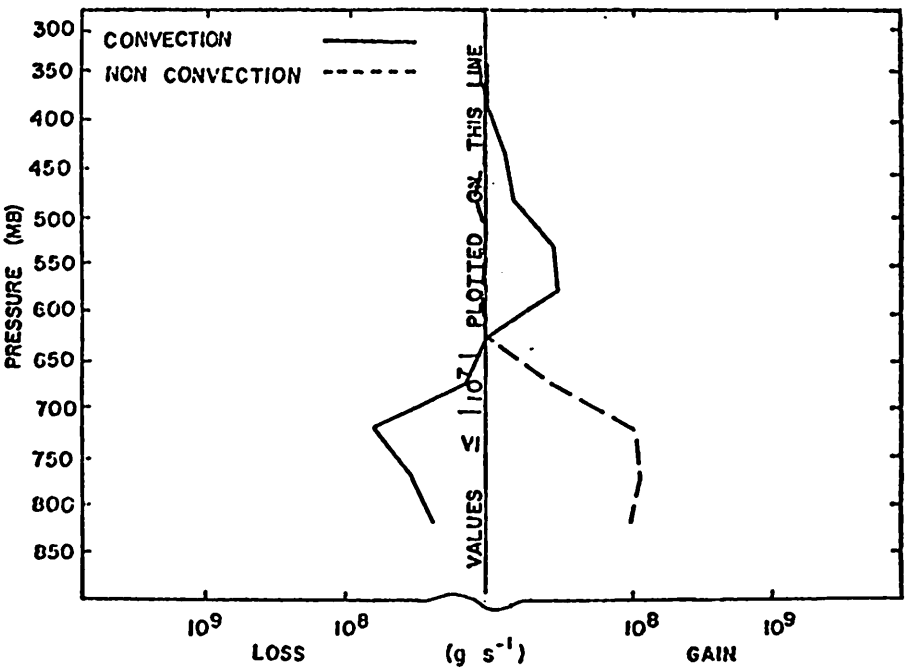

Fig. 7. Local rate-of-change in the total mass of water vapor (g s^{-1}) over the Texas HIPLEX area for average convective and non-convective cases.

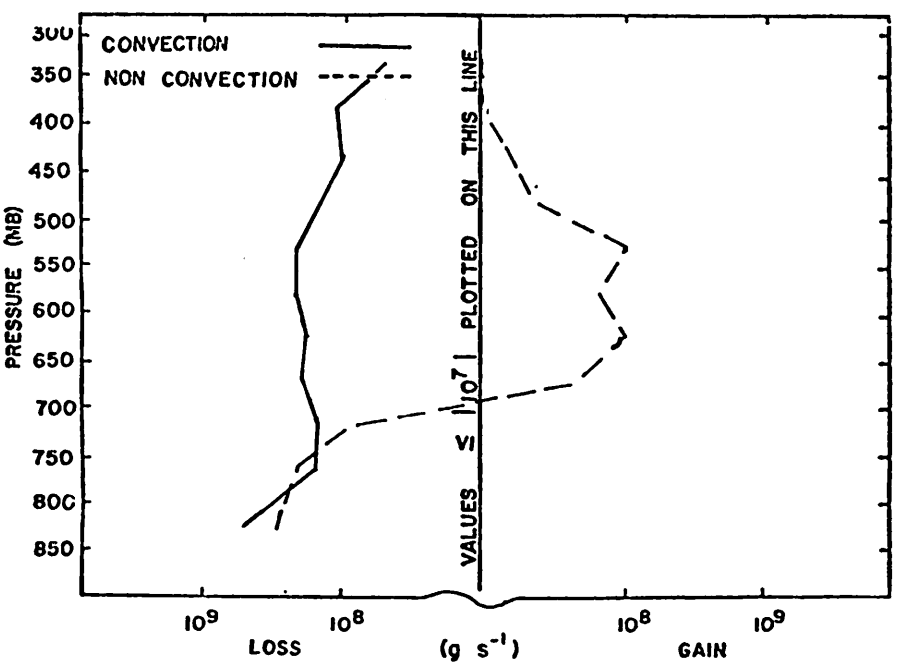

Fig. 8. Residual term of the water vapor budget for 50-mb layers in (g s^{-1}) over the Texas HIPLEX area for average convective and non-convective cases.

The vertical transport of water vapor through constant pressure surfaces (Fig. 4) shows differences for convective and nonconvective cases. A strong upward transport is seen at all levels for cases of convection. This indicates upward motion at all levels since the direction of transport is a direct function of the vertical motion. The maximum upward transport occurs in the subcloud layer and may reflect the transport of water vapor converged by the horizontal transport (Fig. 3) into the cloud. In contrast, a downward transport is observed at all levels for non-convective cases. The maximum transport occurs at approximately 750 mb and decreases closer to the surface. This is indicative of a strong downdraft or subsidence especially near cloud base which decreases towards the surface. Also the magnitudes of water vapor transports are at times over an order of magnitude smaller than for convective cases. This can be attributed to an increased water vapor supply and stronger vertical motion associated with convection.

The gain of water vapor near cloud base and aloft for cases of convection is shown by the net vertical transport of water vapor (Fig. 5). For cases of nonconvection the opposite is seen. A net loss in the vertical at approximately 750 mb and a net gain near the surface results. This is due to downward transport of water vapor from upper to lower layers. A net loss of water vapor aloft would inhibit any deep growth of convective activity.

The combined net horizontal and vertical transport of water vapor is shown in Fig. 6. A strong net inflow is seen for all layers during convective cases. These magnitudes show little variation with height with a maximum net convergence occurring in subcloud layers. Strong net convergence aloft is due to gain of water vapor from both the horizontal (Fig. 3) and vertical (Fig. 5) transports. For nonconvective cases a net gain is seen up to 750 mb with divergence aloft. Again, the magnitude of water vapor transport for convective cases in subcloud layers exceeds that for non-convective cases. By comparison of these profiles it is evident that the moisture source for deep convection occurs above cloud base in addition to near the

surface. Water vapor from subcloud layers may be the principal moisture source during early stages of convective activity but a larger inflow above cloud base is needed to develop and sustain deep convection.

Profiles of the average local rate-of-change in the total mass of water vapor (Fig. 7) shows great differences between convective and nonconvective cases. For convective cases a net loss is observed below 650 mb and a net gain above. Small changes in water vapor occur above 650 mb for non-convective cases. This can be attributed to the lack in total mass of water vapor aloft, and its subsequent transport. However, a substantial gain of water vapor in the lower layers results due to the downward water vapor transport shown in Fig. 4. The maximum loss and gain of water vapor for convective and nonconvective cases, respectively, occurs approximately at cloud base and in subcloud layers.

The residual term in the water vapor budget (Fig. 8) shows a net loss at all layers for convective cases. The largest magnitudes occur below 500 mb. The source of precipitation probably is in this layer, where maximum water vapor convergence exists. For non-convective cases, the residual contributes to a gain above 700 mb which offsets the loss of moisture due to the horizontal and vertical divergence of water vapor. Below 750 mb both profiles show little difference. The similarity of the nonconvective profiles in low layers might indicate the formation of "fair weather" cumulus which would not develop vertically and glaciate due to the entrainment of dry air aloft.

In summary, convective and nonconvective cases indicate large differences between profiles especially above cloud base. Little difference is seen in subcloud layers, which indicates that the moisture source responsible for convective activity occurs above cloud base. For nonconvective cases there is very little accumulation of moisture at levels corresponding to cloud development (Fig. 7). This indicates that water vapor is an important energy source in the development and maintenance of convective activity.

b. Isolated, clusters, and lines of convective cells

Large differences in water vapor processes exist between several classifications of convective activity shown in Figs. 9-14. The net horizontal transport of water vapor (Fig. 9) shows a large inflow at all layers for clusters of cells. This profile basically resembles that for all cases of convection which shows a large net gain in water vapor both near the surface and at 600 mb. The profile for lines of cells also shows a large net gain both near the surface and between 650 mb and 500 mb. The profile for cases of isolated cells shows a net loss near 750 mb and 500 mb. A comparison of profiles for various types of convective activity indicates large changes with height in the net horizontal transport of water vapor especially for isolated cells. However, the size and number of these cells could introduce variation in determining the profile for isolated cell cases. A similar net horizontal gain in water vapor occurs at approximately 650 mb for all cases which indicates a water vapor source which is independent of the type of convection involved.

The vertical transport of water vapor through constant pressure surfaces (Fig. 10) shows strong upward transport for clusters and lines of cells. In fact lines of cells exhibit a slightly larger upward transport at all levels than clusters of cells. This might be attributed to an interaction and organized lifting between cells within the line. Yanai et al., (1973) determined that shallower non-precipitating clouds transfer water vapor aloft to support neighboring precipitating ones. The profile for cases of isolated cells again shows large variation with height, with weaker water vapor transports than cases of clusters and lines of cells.

Profiles of net vertical transport of water vapor (Fig. 11) show greater variation than the net horizontal transport. The profile for lines of cells still shows the greatest net gain especially at 700 mb and above 500 mb. The same is true for clusters of cells, but to a lesser magnitude. For cases of isolated cells, a larger net gain is observed near the surface with divergence aloft below 550 mb which is similar to the profile for nonconvective cases (Fig. 5). The

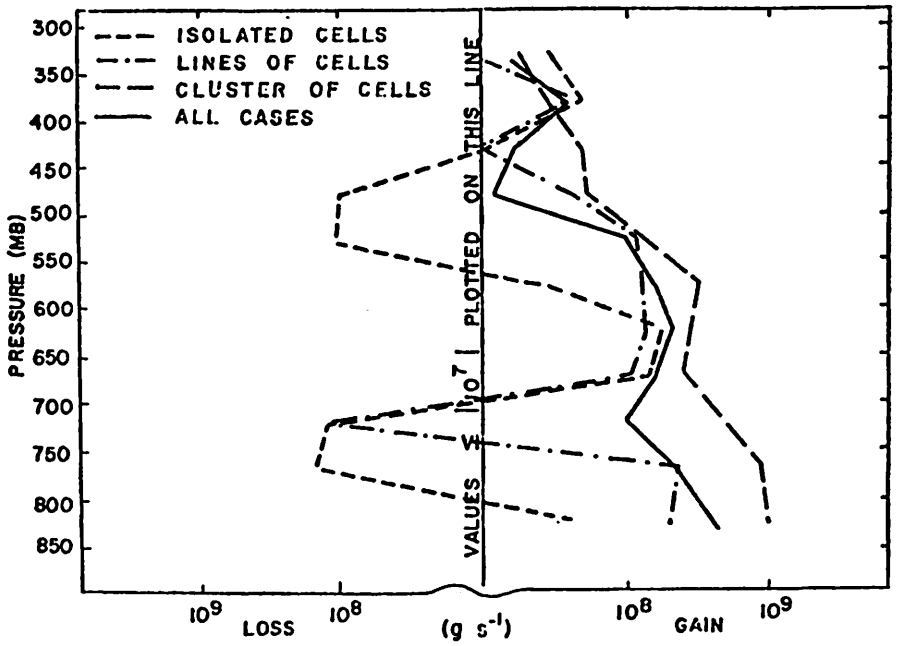

Fig. 9. Net horizontal transport of water vapor through boundaries of 50-mb layers in (g s^{-1}) over the Texas HIPLEX area averaged for types of convective activity.

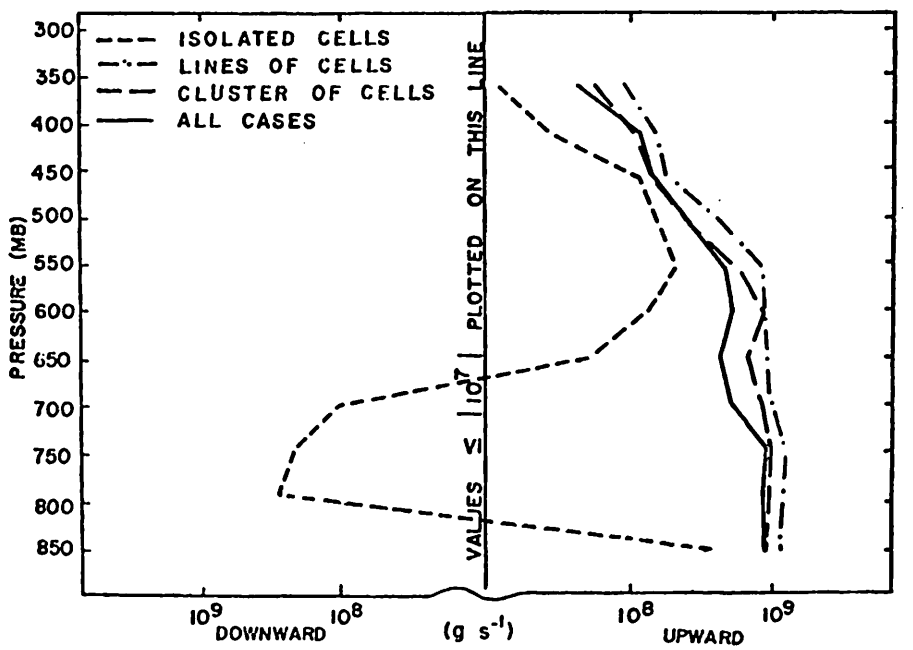

Fig. 10. Vertical transport of water vapor through constant pressure surfaces in (g s^{-1}) over the Texas HIPLEX area averaged for various types of convective activity.

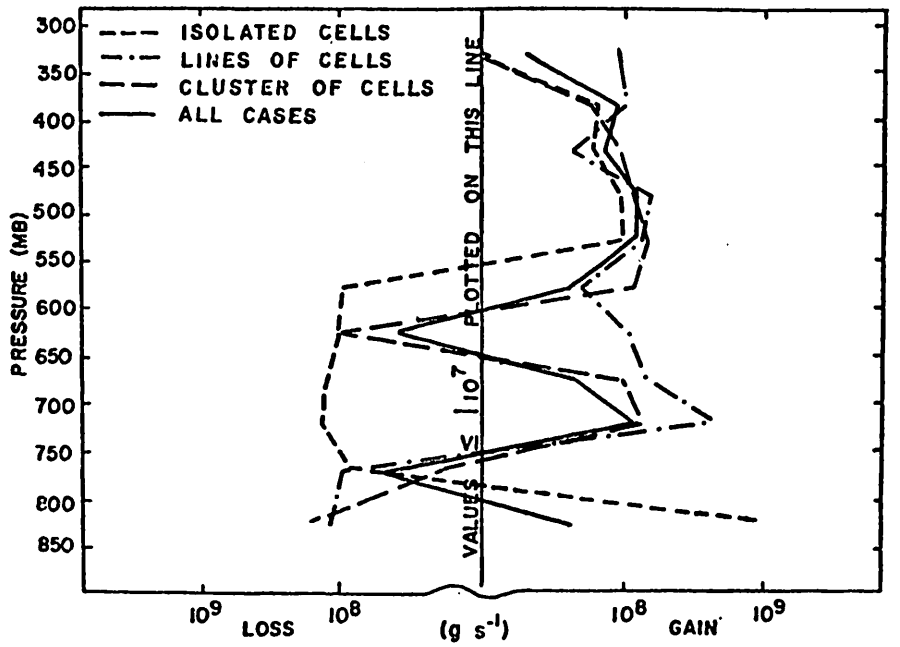

Fig. 11. Net vertical transport of water vapor through boundaries of 50-mb layers in (g s^{-1}) over the Texas HIPLEX area averaged for types of convective activity.

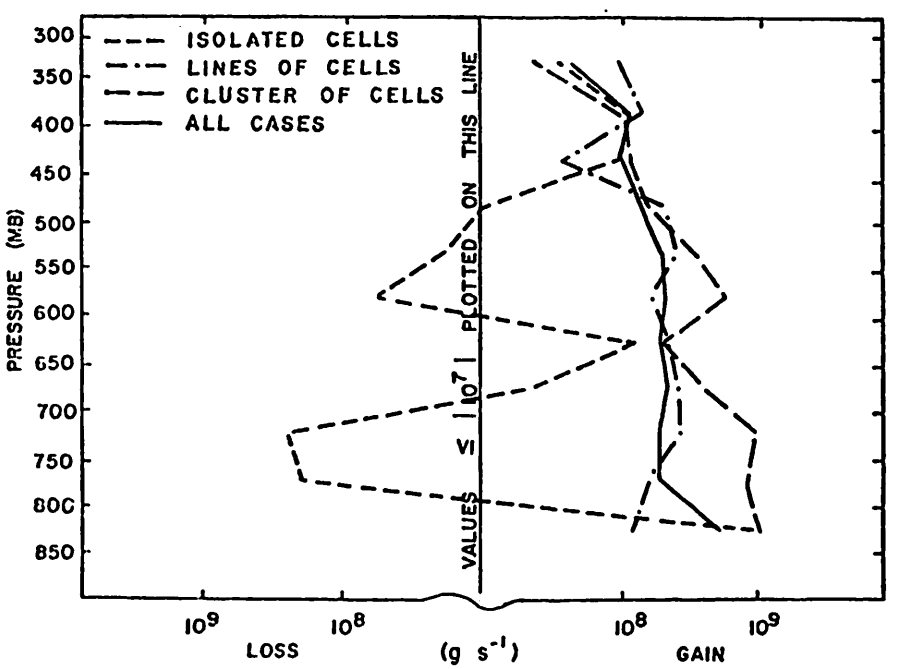

Fig. 12. Combined net horizontal and vertical transport of water vapor through boundaries of 50-mb layers in (g s^{-1}) over the Texas HIPLEX area averaged for types of convective activity.

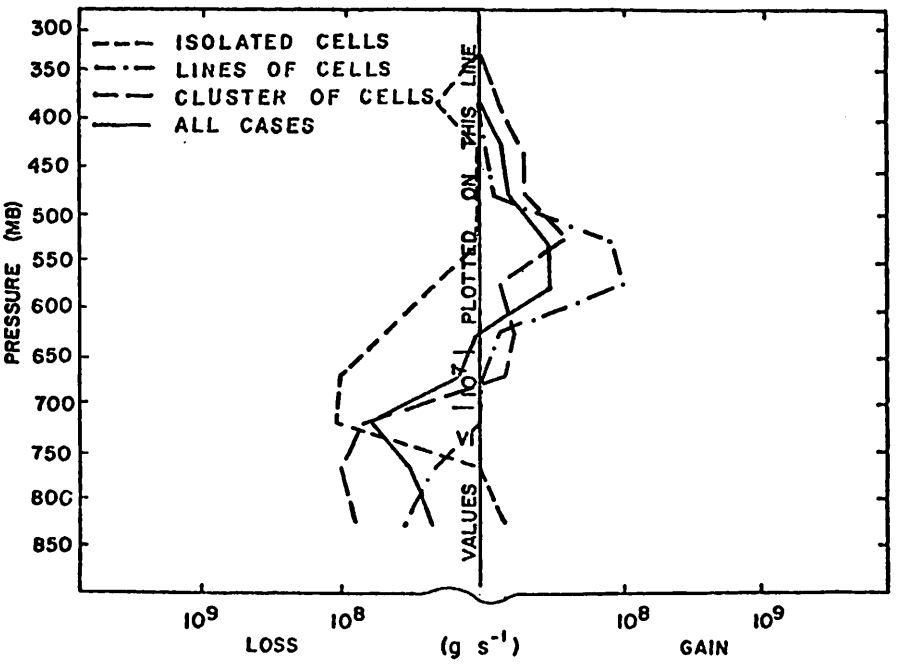

Fig. 13. Local rate-of-change in the total mass of water vapor in 50-mb layers (g s^{-1}) over the Texas HIPLEX area averaged for types of convective activity.

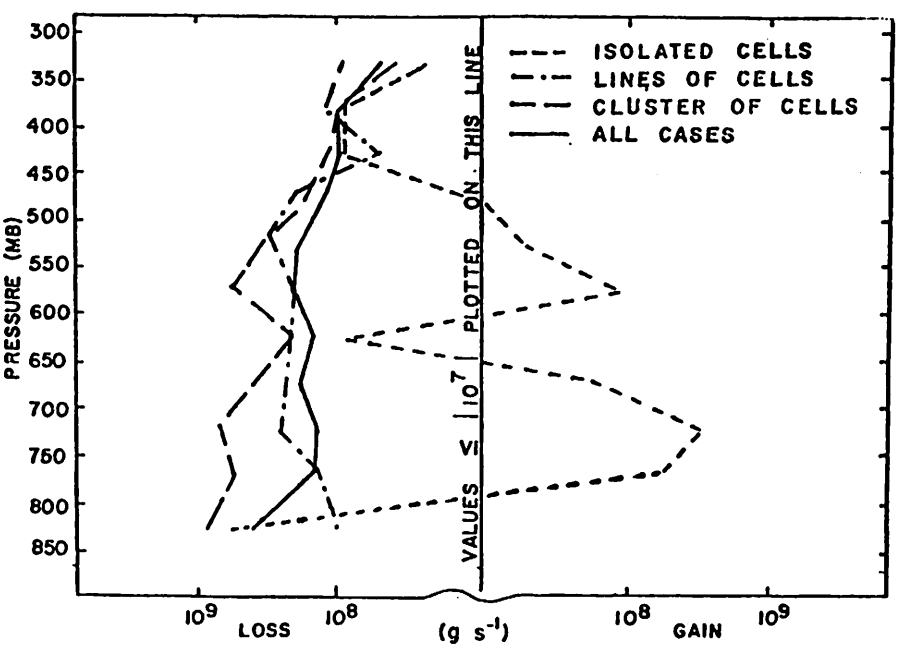

Fig. 14. Residual term of the water vapor budget for 50-mb layers in (g s^{-1}) over the Texas HIPLEX area averaged for various types of convective activity.

profiles for all types of convective activity are similar above 500 mb with the largest differences being near 700 mb. The major difference is that the source of water vapor for isolated cells occurs in subcloud layers while for lines and clusters of cells it is above 700 mb.

Profiles of the combined net horizontal and vertical transports of water vapor are shown in Fig. 12. These profiles indicate large differences between types of convective activity. Profiles for clusters and lines of cells show the greatest water vapor inflow in all layers. The profile for isolated cells shows the water vapor source to be in subcloud layers, with a net divergence near cloud base. Water vapor transports for isolated cell cases appear variable and smaller in magnitude than for clusters and lines of cells. This indicates the more organized and increased water vapor transport needed to sustain and develop clusters and lines of convective cells.

The local rate-of-change in the total mass of water vapor (Fig. 13) also shows differences for all types of convective activity. The profile for isolated cells shows a net loss in all layers except near the surface. This indicates that no accumulation of water vapor aloft occurs, contrary to cases of lines and clusters of cells. The profiles for lines and clusters of cells basically resemble each other and show a net loss in layers below 650 mb, and a net gain above. The largest accumulation of water vapor occurs between 600 mb and 550 mb for lines of cells. These profiles correspond well with the upward vertical transport of water vapor shown in Fig. 11 and the subsequent gain of water vapor aloft.

Differences between lines, clusters, and isolated cells are also seen in the residual term (Fig. 14) of the water budget. Profiles of lines and clusters of cells resemble one another and show a loss in all layers. The largest losses occur around 550 mb which is approximately the same level of maximum gain seen in the local rate-of-change in water vapor (Fig. 13). This indicates that condensation and perhaps precipitation formation may result at this level due to the gain of water vapor aloft. The isolated cell profile shows a net gain near the surface and a loss for most levels from 800 to 500 mb. A net

loss occurs in a small layer near 600 mb, which may indicate that precipitation formation for isolated cells occurs in a small layer. This layer is smaller and slightly lower than for lines and clusters of cells which indicates that precipitation formation for deeper convection occurs in a deeper layer. Thus, the magnitude of the residual term of the water vapor budget for lines and clusters of convective cells far exceeds that for isolated cells.

In summary, Figs. 9-14 show differences between types of convective activity. Profiles for lines and clusters of cells generally resemble one another which indicates little difference between these cases. However, cases for lines of cells show a better organized vertical lifting and an increased "storage" of water vapor aloft. Clusters of cells have larger water vapor transports than lines or isolated cells. Of all types of convective activity, clusters of cells process the largest amount of water vapor. Isolated cells show a marked difference between lines and clusters of cells. Water vapor transports, accumulation, and the residual are all smaller in magnitude and show greater variation with height. This indicates that isolated cells process less water vapor than lines and clusters of cells. Also, lines and clusters of cells are generally of a larger scale comparable to the area shown in Fig. 1. The size of isolated cells may be an important factor in evaluating water vapor processes on the same scale as clusters and lines of cells and may be responsible for large differences shown in the profiles.

c. Depth of convective echoes

Figures 15 through 20 show models of the water vapor budget as a function of depth of convective cells. Profiles of the net horizontal transport of water vapor are shown in Fig. 15. These profiles are similar and nearly coincident near 600 mb. Small variation in the net horizontal transport also occurs at this level for all types of convective echoes (Fig. 9). As the depth of convective activity increases, the magnitude of the divergence aloft increases. This implies that as convective activity intensifies, circulations within the system also intensify, thus increasing the outflow aloft. This divergence is not seen for cases of cell tops less than 6.1 km since

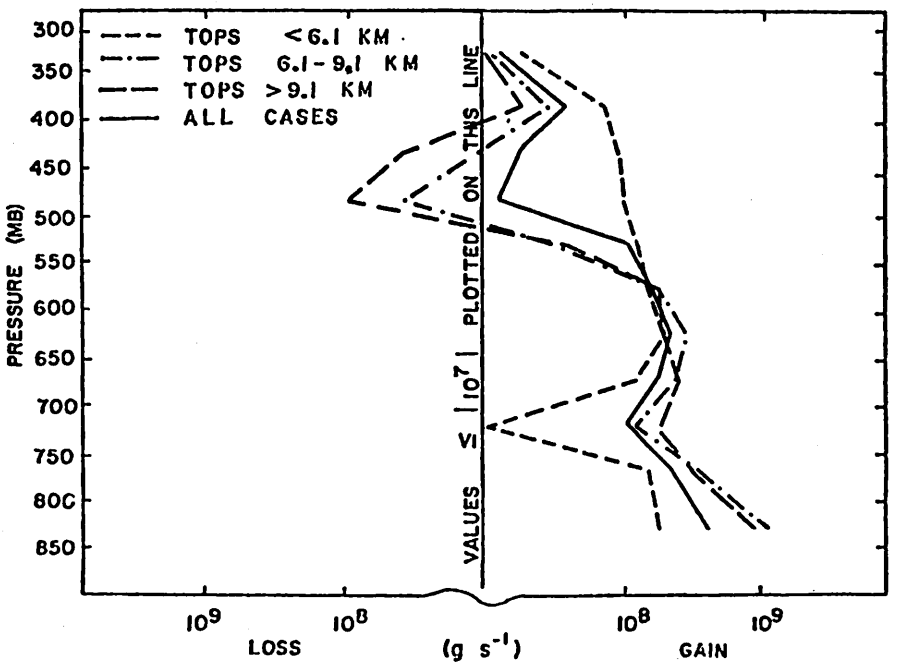

Fig. 15. Net horizontal transport of water vapor through boundaries of 50-mb layers in (g s^{-1}) over the Texas HIPLEX area averaged for various depths of convective activity.

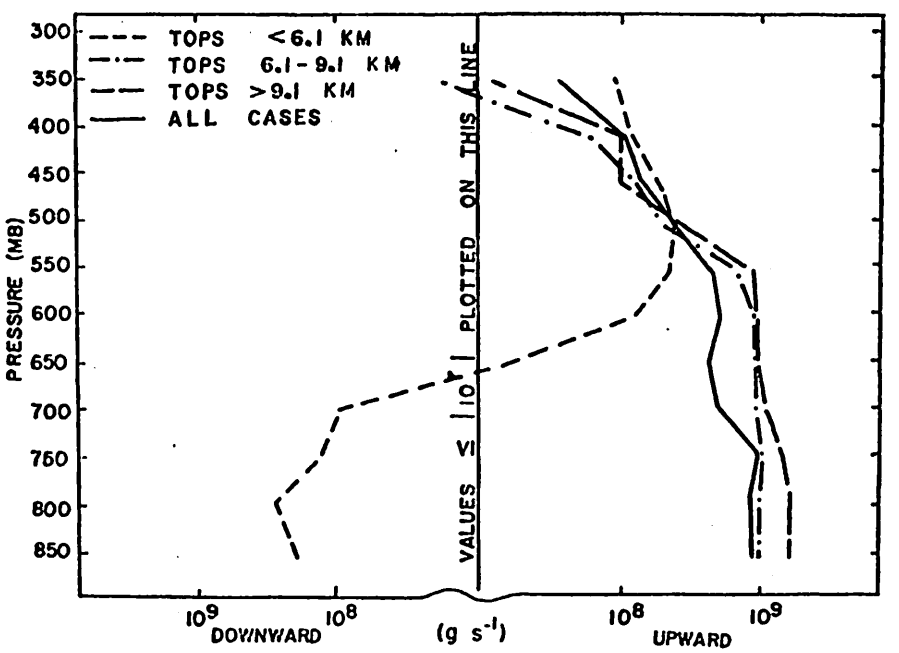

Fig. 16. Vertical transport of water vapor through constant pressure surfaces in (g s^{-1}) over the Texas HIPLEX area averaged for various depths of convective activity.

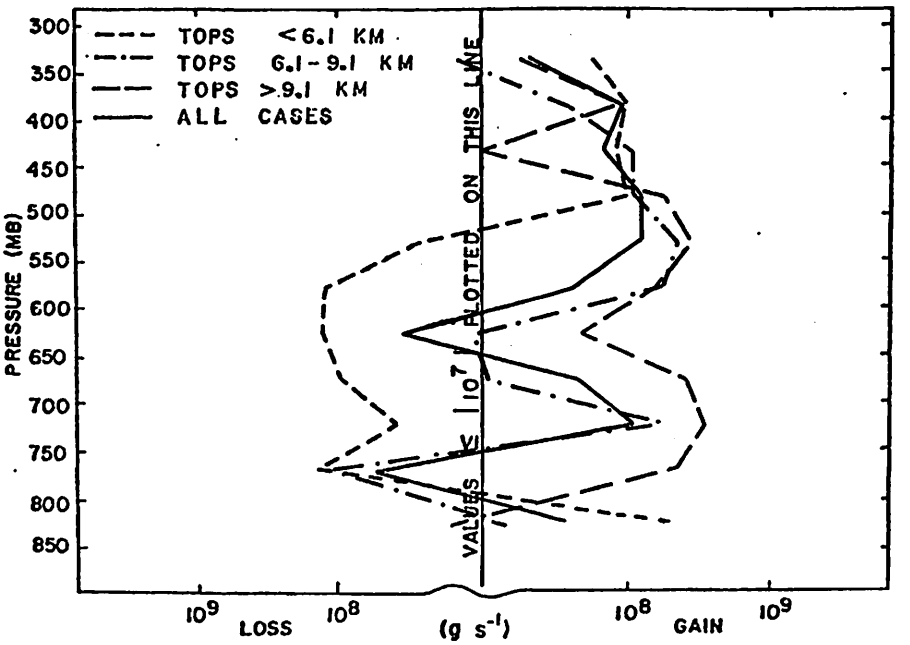

Fig. 17. Net vertical transport of water vapor through boundaries of 50-mb layers in (g s^{-1}) over the Texas HIPLEX area averaged for various depths of convective activity.

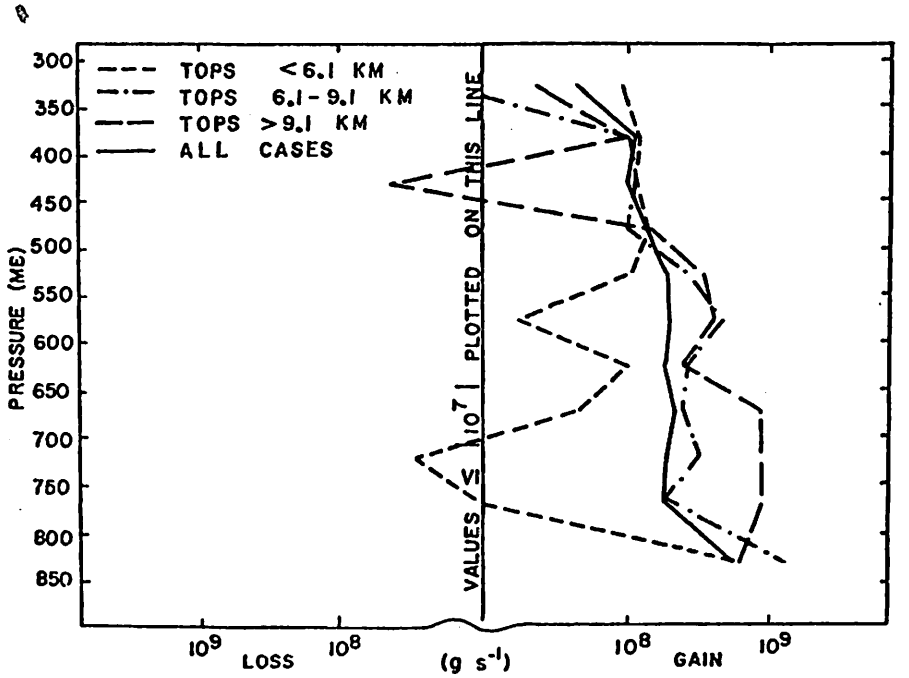

Fig. 18. Combined net horizontal and vertical transport of water vapor through boundaries of 50-mb layers in (g s^{-1}) over the Texas HIPLEX area averaged for various depths of convective activity.

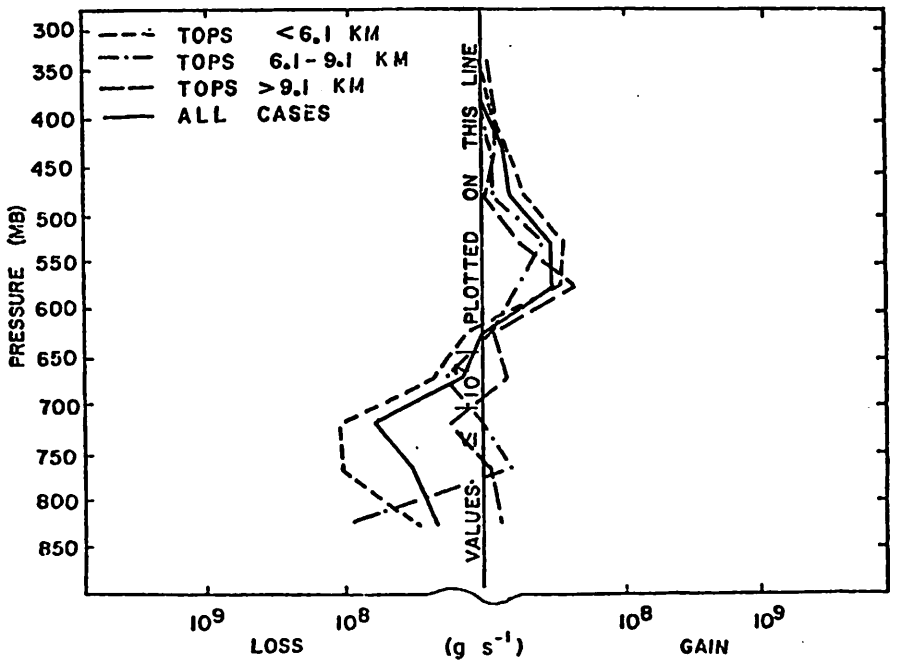

Fig. 19. Local rate-of-change in the total mass of water vapor for 50-mb layers in (g s^{-1}) over the Texas HIPLEX area averaged for various depths of convective activity.

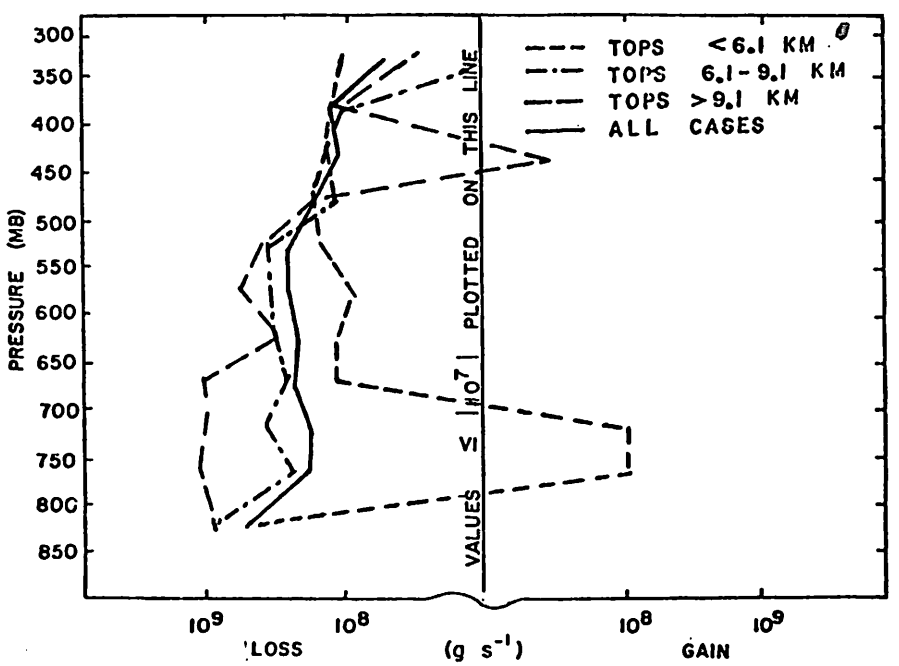

Fig. 20. Residual term of the water vapor budget for 50-mb layers in (g s^{-1}) over the Texas HIPLEX area averaged for various depths of convective activity.

these tops rarely exceed 500 mb. In lower layers, the magnitude of water vapor transport is smaller for cases with tops less than 6.1 km, due to less water vapor processed than by deeper convective activity. Again, as was seen with the type of convection, decreased convergence occurs near cloud base for all cases, especially for cases with tops less than 6.1 km. This might be attributed to increased vertical water vapor transport which dominates the net horizontal transport at this level.

Increased water vapor transports associated with increased depth of convective echoes is also shown in the vertical transport of water vapor through constant pressure surfaces (Fig. 16). Little difference is seen between profiles for tops exceeding 6.1 km. However, for cases of tops exceeding 9.1 km, a slightly larger upward water vapor transport occurs near the surface which indicates the increased upward water vapor transport needed for deeper convection. In all cases, this water vapor transport decreases above 550 mb where little variation between profiles is evident. Slight variation between profiles above 550 mb also was observed between the types of convective activity present. For cases with tops less than 6.1 km, a downward water vapor transport occurs below 650 mb. Its magnitude is smaller than for the other cases due to less water vapor processed and the stronger lifting associated with deeper convection.

Profiles of the net vertical transport of water vapor (Fig. 17) show great differences. For tops less than 6.1 km, a net loss occurs between 800 and 500 mb. This net loss in the vertical could explain the lack of vertical development aloft. Also the water vapor convergence increases as the depth of convective activity increases. For tops exceeding 9.1 km, a strong convergence of water vapor at cloud base occurs. This "accumulation" coupled with a strong upward vertical transport is responsible for transporting subcloud water vapor aloft to support deep convective activity. The deeper the convection, the stronger the net vertical transport at cloud base becomes. This is also true for lines and clusters of cells (Fig. 11), which indicates the importance of this transport in supporting increased

convective growth. Water vapor transports also decrease above 450 mb.

Increased water vapor transports with deeper convection is also shown in the combined net horizontal and vertical transport of water vapor (Fig. 18), especially near the surface. The largest differences between tops exceeding 6.1 km occur below 650 mb which indicates the increased water vapor transport in subcloud layers needed for deeper convection. For cases of tops exceeding 9.1 km, little difference is seen above 650 mb except for a divergent layer around 450 mb. This can be attributed to a stronger outflow aloft shown in the net horizontal water vapor transport (Fig. 15). For tops less than 6.1 km, a decreased combined net gain in the horizontal and vertical occurs in all layers below 500 mb.

Contrary to water vapor transports, the local rate-of-change in the total mass of water vapor (Fig. 19) shows little differences between profiles. These profiles show a similar net gain above 650 mb with a net loss below. A larger net loss is seen in subcloud layers for tops less than 6.1 km.

The residual term in the water budget (Fig. 20) shows an increased net loss for tops exceeding 9.1 km. Largest values are seen in subcloud layers and may be attributed to turbulent transport of water vapor, and at 550 mb from precipitation formation. This increase at 550 mb was also seen for cases of lines and clusters of cells (Fig. 14). Lesser amounts of turbulent transport of water vapor, condensation, and precipitation formation are shown for tops less than 9.1 km. In fact, for tops less than 6.1 km, evaporation is suggested below cloud base due to adiabatic heating of the descending air shown in Fig. 16.

In summary, models for the depth of convective activity show a definite dependence on water vapor processes. As the depth of convection increases, the magnitudes of water vapor transports increase near the surface. Divergence aloft is observed which indicates a circulation within the system that increases with cell depth. The deeper the convection, the greater is the net vertical transport of water vapor near cloud base. Strong upward vertical transport also accompanies strong convective activity.

d. Areal coverage of convective echoes

Figures 21-26 show the relationship of the water vapor budget to areal coverage of convective activity over the Texas HIPLEX area.

The net horizontal transport of water vapor (Fig. 21) shows a net gain in all layers for cases of greater than or equal to 50% areal coverage, especially near the surface. This indicates strong net inflow in lower layers for widespread convective activity. For cases of less than 50% areal coverage, a net outflow or divergence occurs in lower layers. These profiles are similar above 650 mb but with differences near cloud base and in subcloud layers.

Profiles of vertical transport of water vapor through constant pressure surfaces (Fig. 22) also show great differences. Strong upward water vapor transport occurs through all levels for cases of areal coverage greater than or equal to 50%. Smaller water vapor transports exist for areal coverage less than 50%. In fact, for these cases a downward transport occurs between 800 and 600 mb which indicates downward motion and possibly subsidence around these cells.

Figure 23 shows profiles of the net vertical transport of water vapor. For cases of areal coverage less than 50%, a net gain occurs below 700 mb, due to the downward transport of water vapor shown in Fig. 22. Above 700 mb, a net loss occurs in most layers. Conversely, for cases of areal coverage greater than or equal to 50%, a net loss is observed in layers below 700 mb, and a net gain above. This is due to strong upward vertical transport (Fig. 22) especially near the surface that is indicative of a "storage" of water vapor aloft accompanying increased convective activity.

The combined net horizontal and vertical transport of water vapor (Fig. 24) show large differences between profiles. A large net gain in all layers accompanies cases of greater than or equal to 50% areal coverage. This large net gain is attributed to a large net horizontal convergence of water vapor (Fig. 21) in lower layers and a net vertical "accumulation" of water vapor aloft (Fig. 23). For cases of less than 50% areal coverage, a deep layer of divergence exists between 550 and 800 mb. The greatest differences between these profiles exist in this layer where moisture processes related to convection are most

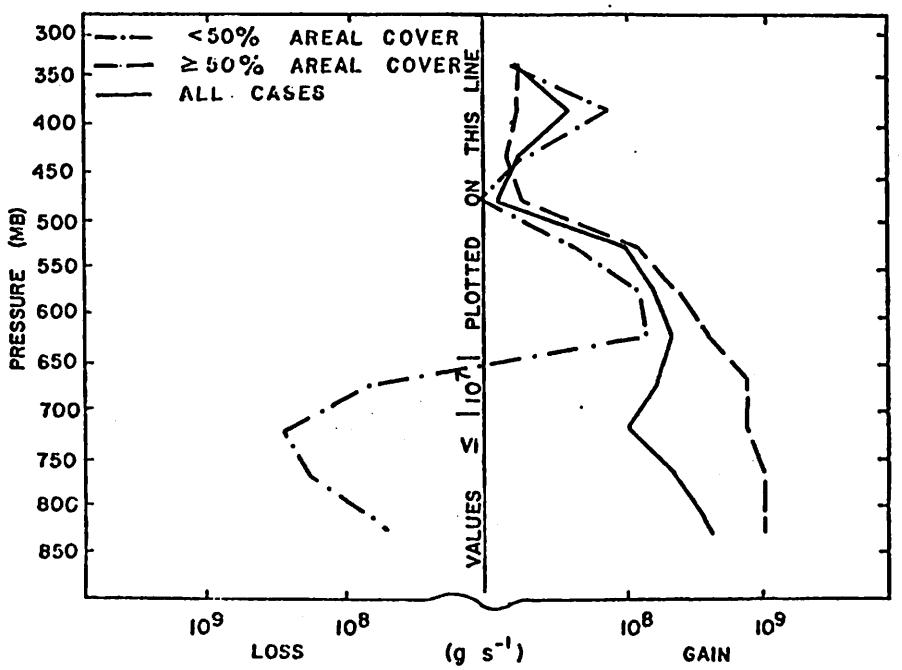

Fig. 21. Net horizontal transport of water vapor through boundaries of 50-mb layers in (g s^{-1}) over the Texas HIPLEX area averaged for areal coverage of convective activity.

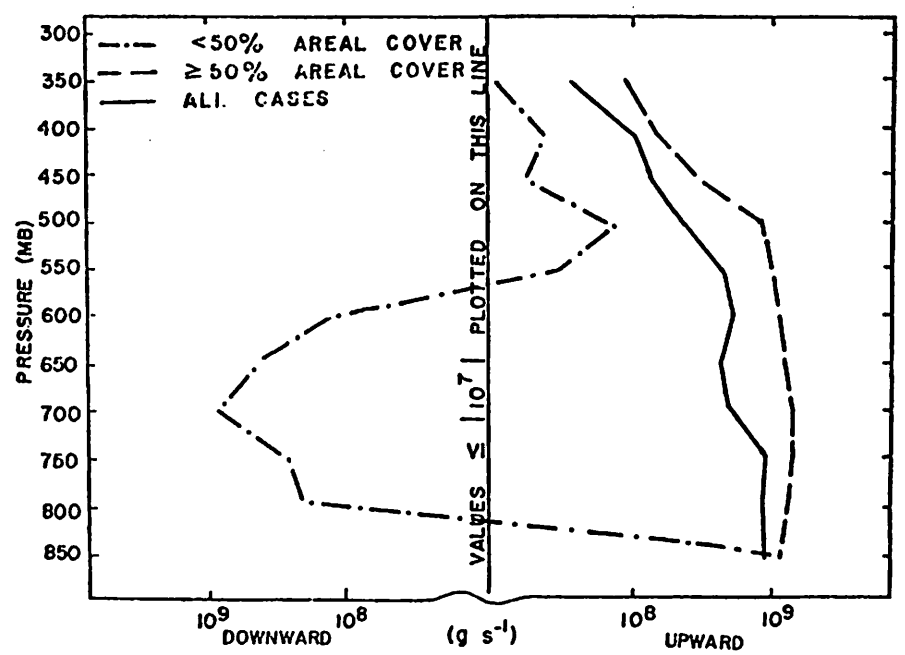

Fig. 22. Vertical transport of water vapor through constant pressure surfaces every 50-mb in (g s^{-1}) over the Texas HIPLEX area averaged for areal coverage of convective activity.

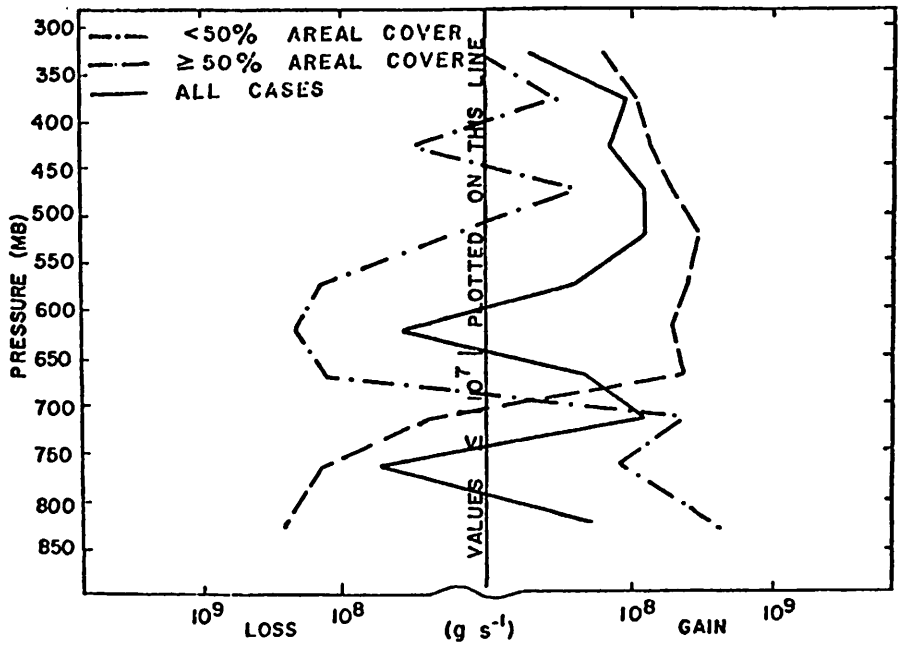

Fig. 23. Net vertical transport of water vapor through boundaries of 50-mb layers in (g s^{-1}) over the Texas HIPLEX area averaged for areal coverage of convective activity.

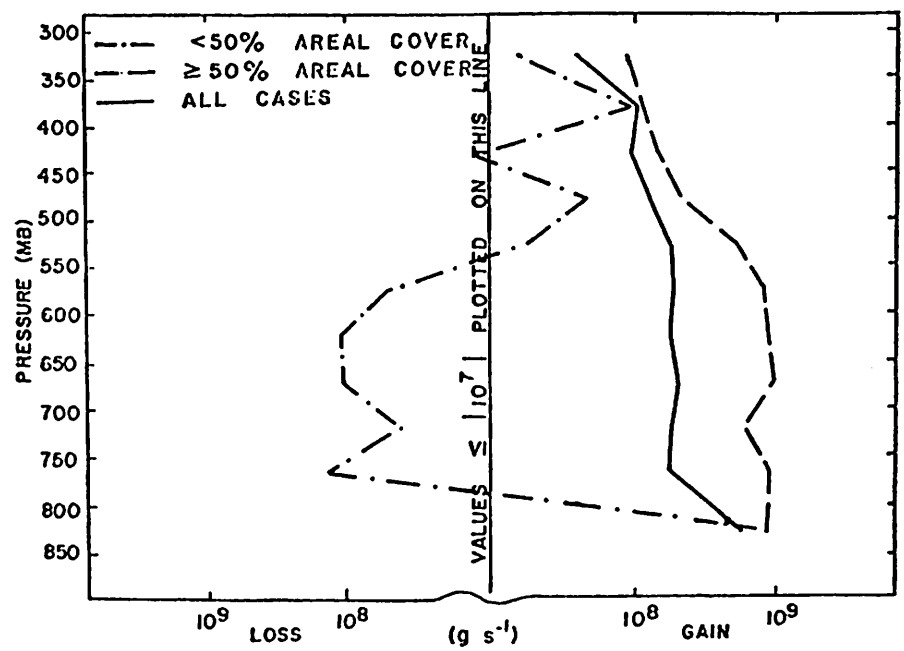

Fig. 24. Combined net horizontal and vertical transport of water vapor through boundaries of 50-mb layers in (g s^{-1}) over the Texas HIPLEX area averaged for areal coverage of convective activity.

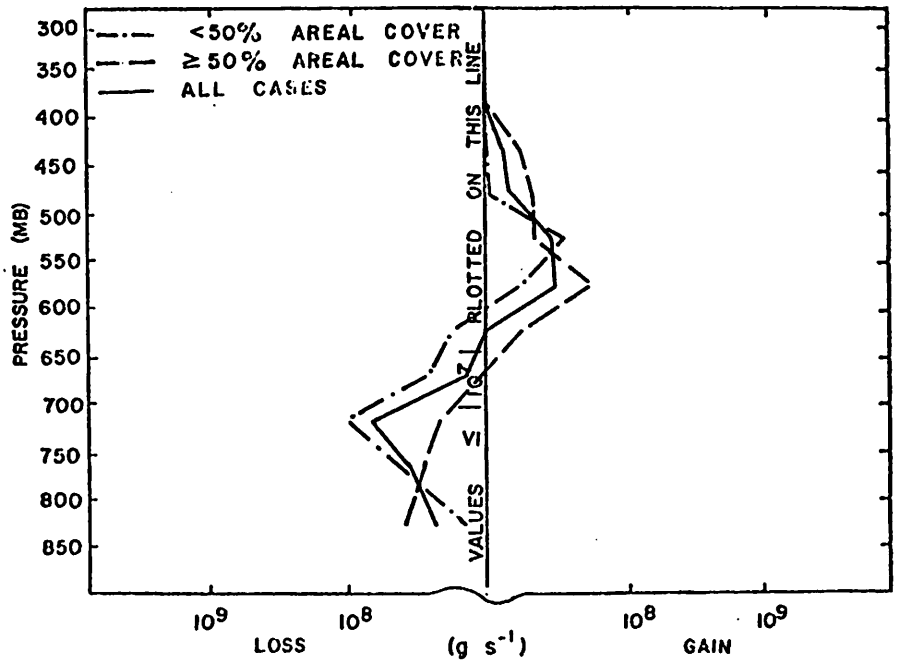

Fig. 25. Local rate-of-change in the total mass of water vapor for 50-mb layers in (g s^{-1}) over the Texas HIPLEX area averaged for areal coverage of convective activity.

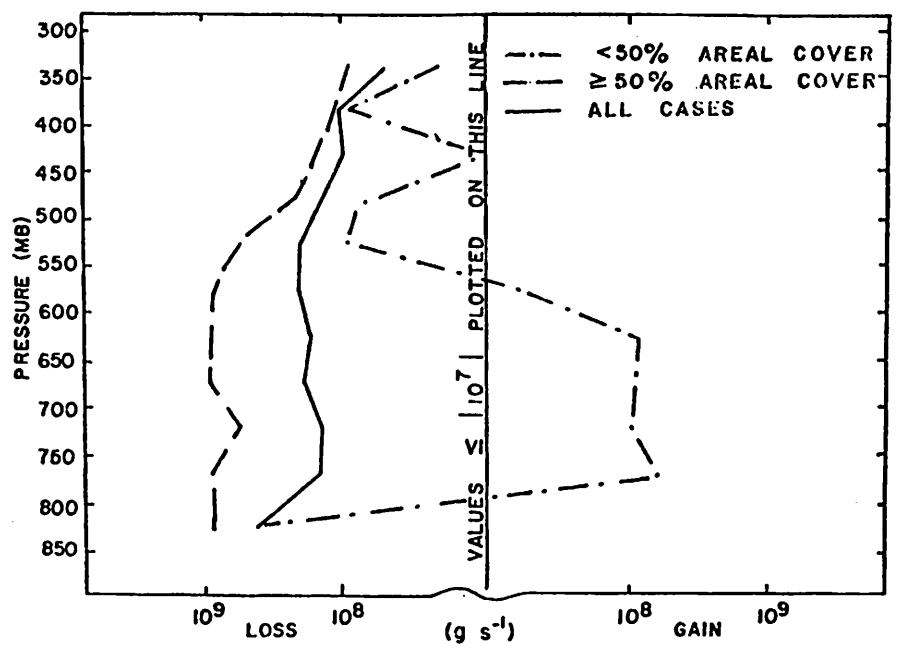

Fig. 26. Residual term of the water budget for 50-mb layers in (g s^{-1}) over the Texas HIPLEX area averaged for areal coverage of convective activity.

important.

The local rate-of-change in the total mass of water vapor (Fig. 25) shows a net loss below 600 mb for areal coverage less than 50%. This net loss is largest near 700 mb. The same pattern holds for cases of areal coverage greater than or equal to 50%. The local rate-of-change profiles for areal coverage do not show the large differences seen in other water vapor budget terms (Figs. 21-24). The local rate-of-change term remains nearly an order of magnitude smaller than other water budget terms.

The residual term of the water budget (Fig. 26) shows greatest differences between profiles below 550 mb. For cases of greater than or equal to 50% areal coverage, a net loss occurs in all layers. For cases of less than 50% areal coverage, a layer of evaporation exists between 800 and 550 mb, with condensation and a net loss of water vapor possibly due to turbulent transport in layers near the surface. Above 550 mb little difference is seen in these profiles.

In summary, a comparison of models as a function of areal coverage of convective echoes shows large differences in water vapor processes. The largest changes occur below 550 mb which implies the importance of widespread areal convection and perhaps the depth of convection. This importance is reflected in Figs. 21-26, and further indicates that the important water vapor processes occur in layers below 550 mb.

e. Comparison of models

The profiles presented showed variation between the presence, type, intensity, and coverage as well as the interaction of moisture processes between various layers. Table 2 shows a comparison of various models to each water vapor budget term summed for each 50-mb layer from 850 to 300 mb. These results demonstrate the relative magnitudes of water vapor processes between all the models.

Strong net gain in horizontal transport of water vapor occurs for each case except for isolated, nonconvective, and less than 50% areal coverage. These differences (over an order of magnitude) indicate the importance of the horizontal transport of water vapor observed in strong, widespread convection. The largest transports occur in cases of areal coverage greater than or equal to 50% and for

Table 2. Inter- and intra-comparisons of terms summed for each 50-mb layer from 850 to 300 mb in the water vapor budget models.

MODEL	STRATIFICATION	WATER VAPOR BUDGET TERMS ($\times 10^8$ g s^{-1})			
		NET HORIZONTAL TRANSPORT	NET VERTICAL TRANSPORT	LOCAL RATE-OF CHANGE	RESIDUAL
Presence	Non-Convective	3.02	-2.38	5.05	-5.69
	Convective	26.70	9.57	-0.57	-35.70
Type	Lines of cells	17.31	19.24	2.17	-38.72
	Clusters of cells	52.54	9.53	-0.37	-61.70
	Isolated cells	1.16	1.88	-4.36	1.32
Depth	Cell tops less than 6.1 km	21.60	-4.95	-2.45	-14.20
	Cell tops between 6.1 and 9.1 km	32.40	14.50	0.35	-47.25
	Cell tops greater than 9.1 km	30.70	31.20	2.16	-64.06
Areal Coverage	Less than 50%	-3.72	1.09	-1.87	4.50
	Greater than or equal to 50%	62.27	21.04	0.94	-84.25

clusters of cells. This seems reasonable since the increased convection would require an increased source of water vapor. Also, it would appear from these results that the horizontal transport of water vapor is greatly dependent on the amount of convection occurring in the area rather than the type or intensity. For example, tops between 6.1 and 9.1 km actually have a greater horizontal convergence of water vapor than do tops greater than 9.1 km. However, this is understandable since the height of a convective cell is due mainly to the amount of water vapor transported in the vertical. This is demonstrated by over 2 times the net vertical transport of water vapor for cases with tops greater than 9.1 km over cases with tops between 6.1 and 9.1 km

inclusive. Also, a larger horizontal transport occurs for non-convective cases than for areal coverage less than 50%. This might be attributed to the formation of "fair weather" cumulus over an area greater than 50% of the HIPLEX area. Although these cells do not grow convectively, the horizontal transport is great enough in these lower layers to result in a total net gain when integrating between 850 and 300 mb.

Values of the net vertical transport of water vapor are appreciably less than the net horizontal transport of water vapor. The largest values are observed with tops greater than 9.1 km and areal coverage greater than or equal to 50%. This indicates a dependence on areal coverage as well as vertical development in the net vertical transport of water vapor. Also, lines of cells show a large vertical transport of water vapor as well. This can be attributed to organized lifting by adjacent cells. Yanai et al. (1973) showed shallower non-precipitating clouds transporting water vapor aloft to neighboring deep precipitating ones. A net loss in water vapor in the vertical occurs in non-convective cases and for tops less than 6.1 km. This net loss in water vapor is largest above cloud base where entrainment of dry air would inhibit any deep convection. However, in summary, for most cases the net vertical transport of water vapor is usually 2 to 3 times smaller than the corresponding net horizontal transport.

Values of the local rate-of-change in the total mass of water vapor also remain very small. The largest net gain is observed for non-convective cases because of a large downward transport of water vapor near the surface. For cases of lines of cells, tops exceeding 6.1 km, and areal coverage greater than 50%, a net gain is observed due to the "storage" of water vapor needed to sustain deep and widespread convection. For all other cases a slight loss was observed. These values are smaller than net horizontal and vertical transports of water vapor.

The residual term in the water vapor budget shows large losses for most models. The largest values occur for cases of areal coverage greater than or equal to 50%, tops exceeding 9.1 km, and clusters of cells. This indicates that the larger the area covered and the deeper

the convection the more condensation and precipitation one would expect. A net gain was found for areal coverage less than 50% and for isolated cells. This might be attributed to convection occurring on too small a scale to be detected by average water vapor processes over the area considered. A slight loss is still seen for non-convective cases which might be attributed to "fair weather" cumulus that form over the area during the day and move out.

8. INTERPRETATION OF THE RESIDUAL TERM IN THE WATER BUDGET EQUATION

In previous sections the residual term was discussed as an integral term of the water vapor budget. However, no attempt to examine individual components comprising the residual term was made. On days when precipitation is recorded a quantitative comparison of precipitation to condensation, evaporation, and the turbulent transport of moisture through the boundaries comprising the residual term can be made.

a. Method of data analysis

Sounding data taken at 3-h intervals from 1500 to 0300 GMT on 22-23 June, and 10-11 July 1976 were analyzed on a case study basis. Each term in Eq. (5) was evaluated for the entire triangular volume constructed from the area shown in Fig. 1 times the vertical distance between 850 and 300 mb. The results of the four water vapor budget terms in units of ($g\ s^{-1}$) for both days are shown in Figs. 27 and 28. Times when radar echoes over the Texas HIPLEX area, and when precipitation was recorded within the Texas HIPLEX network, are also denoted.

Hourly totals of precipitation were provided by the Bureau of Reclamation for an area of approximately $4.096 \times 10^9\ m^2$ (see Fig. 29). This area is approximately half the size of the triangular area. Hourly totals of precipitation obtained in units of acre-feet were converted to cubic centimeters and are shown for their respective times in Table 3. A conversion from cubic centimeters to grams was made utilizing the density of water.

The residual term of the water vapor budget equation computed over the Texas HIPLEX area was linearly interpolated from Figs. 27 and 28 for the times for which precipitation data were available.

Hourly totals of the residual term in equivalent grams of water were obtained by linearly interpolating Eq. (5). The residual term was reduced in magnitude (normalized) by the ratio of the area for which total precipitation was determined to the area of the triangle formed by the rawinsonde stations (see Fig. 29). This normalized residual term was then compared with the measured total precipitation

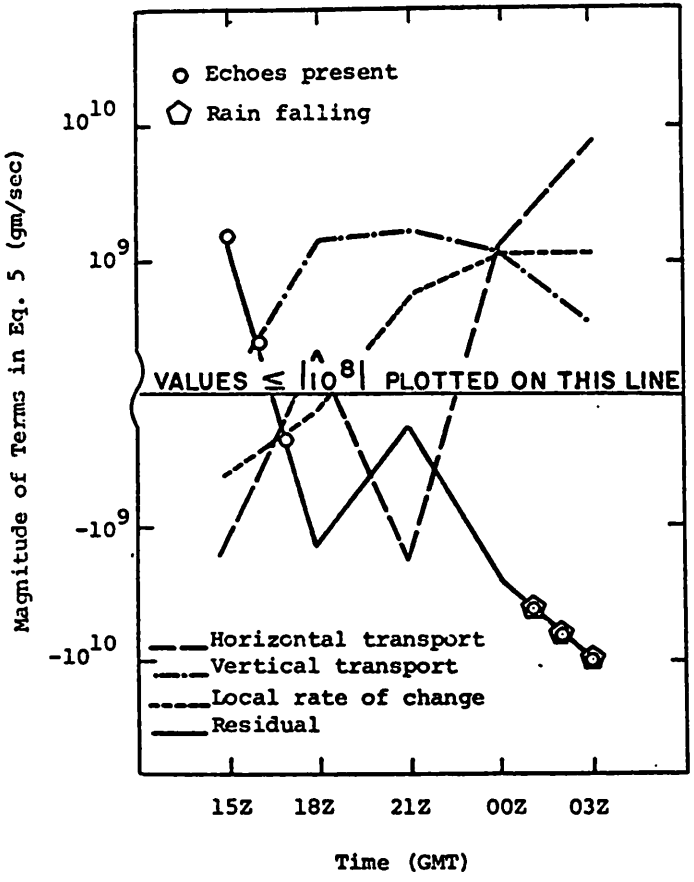

Fig. 27. Comparison of terms in the water budget equation for sounding times on 22-23 June 1976.

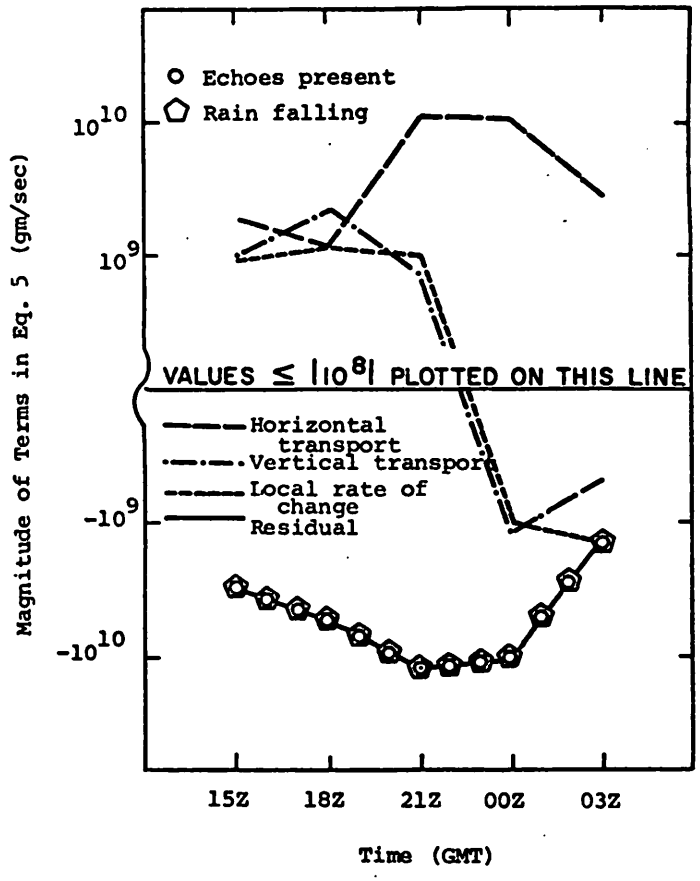

Fig. 28. Comparison of terms in the water budget equation for sounding times on 10-11 July 1976.

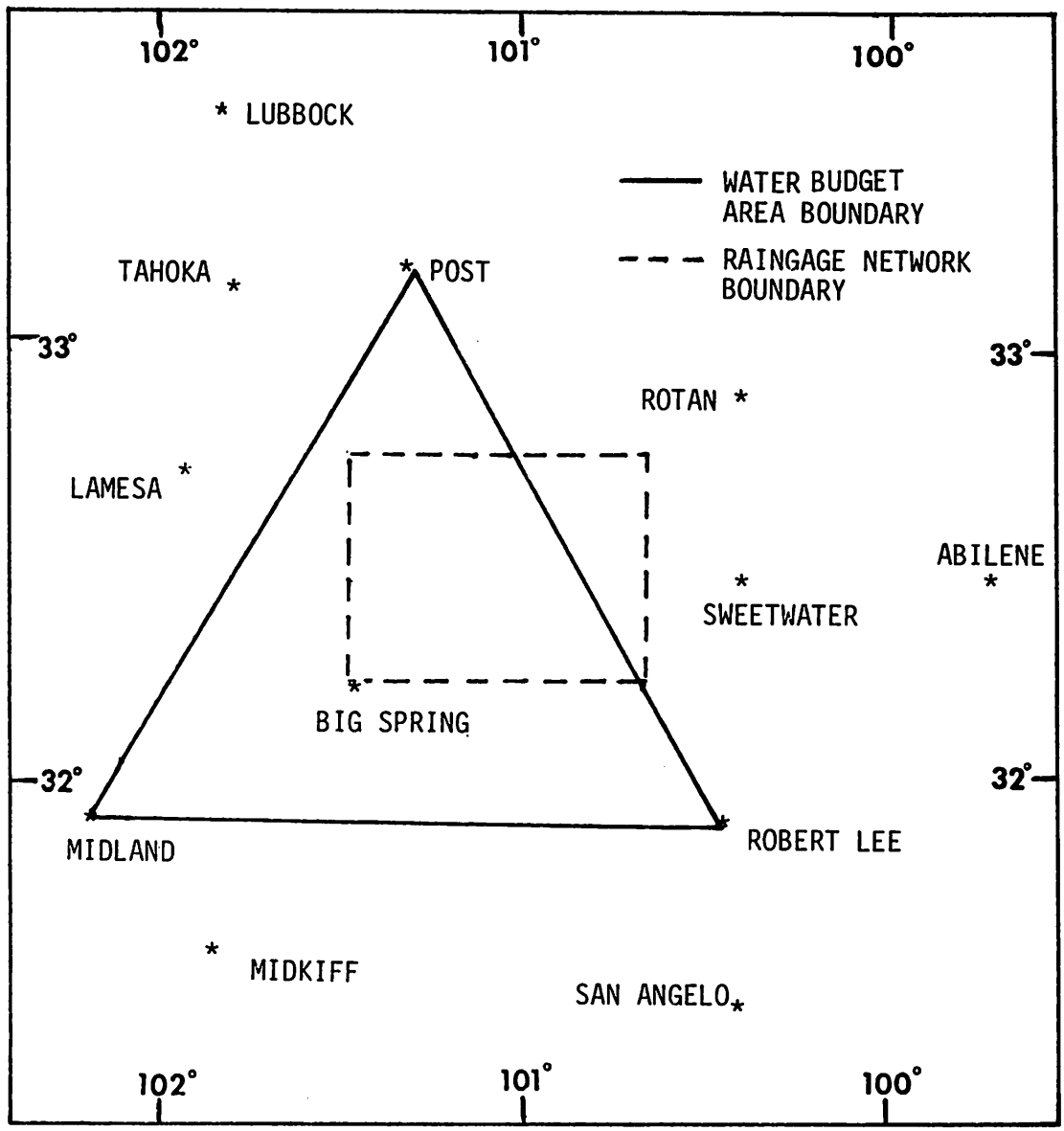

Fig. 29. Triangular area formed by rawinsonde stations and rectangular area for which precipitation data are available.

Table 3. Precipitation amounts, computed residual term, and the ratio of the residual term to precipitation for 1-h periods on 23 June and 10-11 July 1976.

Time (GMT)	Total Precipitation Amount ($\times 10^{12}$ cm^3)	Total Residual Amount ($\times 10^{12}$ cm^3)	Ratio $\frac{R\Delta t(g)}{Precip.(g)}$
	23 June 1976		
01-02	.98	13.3	13.5
02-03	1.84	16.6	9.0
03-04	1.31	17.7	13.5
	10-11 July 1976		
20-21	1.98	21.4	10.8
21-22	3.74	28.4	7.6
22-23	12.30	24.6	2.0
23-00	2.86	21.5	7.5
00-01	1.05	15.3	14.6

for each hour. The ratio of the residual term linearly interpolated over 1-h intervals to total precipitation is shown in Table 3. Both the hourly normalized residual term and the total hourly precipitation were integrated over a 3-h period from 2100 to 0000 GMT on 10-11 July 1976, and the ratio of these terms computed. These results are shown in Table 4.

b. Discussion of results

A comparison of the terms in the water vapor budget with precipitation reveals the source of moisture for the precipitation. Previous results indicate that the horizontal transport of water vapor into an area of convective activity is the primary moisture source. Results shown in Figs. 27 and 28 indicate a substantial increase in the horizontal transport of water vapor during precipitation periods. Both the horizontal transport of water vapor and the residual terms show the

Table 4. Precipitation amounts, computed residual term, and the ratio of the residual term to precipitation for a 3-h period on 10-11 July 1976.

Time (GMT)	Total Precipitation Amount ($\times 10^{12}$ cm^3)	Total Residual Amount ($\times 10^{12}$ cm^3)	Ratio $\frac{R\Delta t(g)}{\text{Precip.}(g)}$
21-00	18.9	74.5	3.9

same trend, especially during periods of precipitation. The relative magnitudes of other terms in the water vapor budget remain small or insignificant during periods of precipitation. These results agree favorably with those of Palmen et al., (1962) in which the horizontal transport term far exceeded other terms during precipitation periods.

When precipitation is large, one would expect the ratio of the residual term to total precipitation amount over a 1-h period to be smaller than when precipitation is small. This is because precipitation should account for more of the condensation contribution in the residual term. This relationship is shown by the results in Table 3. Also as the integration period increases, the contributions by condensation and evaporation to the residual term should tend to make precipitation the dominant factor in the residual term (assuming turbulent boundary fluxes remain unchanged or insignificant). In the limit when the residual term is determined for a large area and over long time periods, precipitation should account for a large part of the condensation and the ratio should approach unity. The fact that the ratio decreases as the integration time increases is shown in Table 4. The ratio for the 3-h period shown in Table 4 is 3.9, and for 1-h periods shown in Table 3 it varies between 2.0 when precipitation amounts were large to 7.6 when precipitation was moderate.

Results have shown that trends of both the residual term and actual recorded precipitation closely resemble each other. However, comparison of the magnitudes of these values indicates a large over-compensation

of the residual term is consistently observed for each time period from Tables 3 and 4. Such bias in the results suggests other factors influencing the residual term might be responsible. Condensation of cloud water which is never totally converted to precipitation and the turbulent flux of moisture through the boundaries contribute to an increase in the residual term. Precipitation might never be recorded at the surface due to evaporation taking place between the surface and 850 mb. Condensation and liquid water formation within the triangular area and accounted for by the residual term could be transported out of this area by clouds, resulting in precipitation occurrence in other areas. Also, the slight overlap between the triangular area and the raingage area shown in Fig. 29, as well as the normalization of the residual term to the smaller area, might influence the comparison. If all these factors contributed to increasing the residual term, an observed bias could be substantiated.

9. CONCLUSIONS

Inter- and intra-comparisons of the water budget models for the Texas HIPLEX area have shown definite differences which indicate the variability of environmental response to various forms of convective activity. Outlined below are conclusions based upon this research.

a. Presence of convective cells

1) Largest differences in water vapor transport between cases of convective cells present and the absence of convective cells exist above cloud base (approximately 750 mb). A strong net gain of water vapor in all cloud layers exists for cases of convective activity, whereas a net loss in these same layers occurs for cases of non-convection. In sub-cloud layers similar net gains in water vapor exist for both cases which indicates the importance of water vapor inflow aloft to support convective activity.

2) Water vapor transport magnitudes are larger for convective than nonconvective cases in all layers.

b. Type of convective cells

1) Water vapor transports for cases of lines and clusters of convective cells are similar. However, lines of cells exhibit a stronger lifting and, therefore, increased transport of water vapor in the vertical. Conversely, cases for clusters of convective cells show a larger combined net horizontal and vertical transport of water vapor which indicates a greater amount of water vapor is processed than for lines of cells, leading to larger precipitation amounts.

2) Cases for isolated convective cells do not exhibit the same organized water vapor transport associated with cases of lines and clusters of convective cells. Thus water vapor transport and accumulation of water vapor in cases of isolated cells are noticably smaller than for lines and clusters of cells.

c. Depth of convective cells

1) As the depth of convection increases, so does the magnitude of water vapor transport near the surface. This indicates that more water vapor is required to support deeper convection. Also, as the depth of convection increases, so does the upward transport of water vapor from

lower layers. Thus, the increased upward transport compliments the increased inflow near the surface as convective activity grows.

2) As the depth of convection increases, so does the horizontal outflow of water vapor near cloud top. Such increased outflow results from an increased upward water vapor transport indicative of stronger circulations within the cells for deeper convection.

d. Areal coverage of convective cells

As the areal coverage of convective cells increases, so does the convergence of water vapor especially near the surface. In order to sustain widespread convective activity, a large supply of water vapor in surface layers is needed. Above 550 mb, no relationship between water vapor transport and areal coverage of convective cells could be made, illustrating that important water vapor processes occur below this level.

e. Comparisons of water budget models

Comparisons of the water budget models show that the greatest amount of water vapor is processed by increased depth and coverage of convective activity. Thus, the amount of convection seems to be more important than the type or presence of convective activity. An increased convergence of water vapor near the surface is also an important factor for increased convective activity. A "storage" of water vapor aloft was also observed to correlate with cases of increased precipitation.

f. The residual term of the water budget

1) A comparison of all the terms in the water budget indicates that the net horizontal transport of water vapor exceeds other terms in the equation as being the primary moisture source for all cases of convection. At times, the local rate-of-change and net vertical transport terms were much smaller in magnitude leaving the net horizontal transport term nearly balancing the residual term. This is especially true during periods of precipitation, making the net horizontal transport term the main source of water vapor for the precipitation.

2) Interpretation of the residual term reveals that during periods of heavy precipitation, precipitation nearly comprises the residual

term. However the water budget consistently overestimated actual precipitation which indicates that cloud water is never totally converted to precipitation. A nearly linear relationship between recorded precipitation and the residual term demonstrates that the amount of precipitation is related to the amount of condensation by nearly a constant factor.

REFERENCES

Auer, A. H., Jr. and J. D. Marwitz, 1968: Estimates of air and moisture flux into hailstorms on the high plains. J. Appl. Meteorol., 7, 196-198.

Bradbury, D. L., 1957: Moisture analysis and water budget in three different types of storms. J. Meteor., 14, 559-565.

Braham, R. R., Jr., 1952: The water and energy budgets of the thunderstorm and their relationship to thunderstorm development. J. Meteor., 4, 227-242.

Fankhauser, J. C., 1969: Convective processes resolved by a mesoscale rawinsonde network. J. Appl. Meteorol., 8, 778-797.

Foote, G. B., and J. C. Fankhauser, 1973: Airflow and moisture budget beneath a northeast Colorado hailstorm. J. Appl. Meteorol., 12, 1330-1353.

Fritsch, J. M., 1975: Synoptic-mesoscale budget relationships for a tornado producing squall line. Preprints of the 9th conference on severe local storms, Norman, Oklahoma, 165-172.

_____, C. F. Chappell, and L.R. Hoxit, 1976: The use of large scale budgets for convective parameterization. Mon. Wea. Rev., 104, 1408-1418.

Fuelberg, H. E., 1974: Reduction and error analysis of the AVE II pilot experiment data. NASA Contractor Report CR-120496. Marshall Space Flight Center, Alabama, 140 pp.

Haltiner, G. J., and F. L. Martin, 1957: Dynamical and Physical Meteorology, New York, McGraw-Hill, 470 pp.

_____, 1971: Numerical Weather Prediction, New York, Wiley, 317 pp.

House, D. C., 1960: Remarks on the optimum spacing of upper air observations. Mon. Wea. Rev., 88, 97-100.

Hudson, H. R., 1971: On the relationship between horizontal moisture convergence and convective cloud formation. J. Appl. Meteorol., 10, 755-762

Krishnamurti, T. N., 1968: A calculation of percentage area covered by convective clouds from moisture convergence. J. Appl. Meteorol., 7, 184-195.

Lewis, J. M., Y. Ogura, and L. Gidel, 1974: Large scale influences upon the generation of a mesoscale disturbance. Mon. Wea. Rev., 102, 545-560.

McNab, A. L., and A. K. Betts, 1978: A mesoscale budget study of cumulus convection. Mon. Wea. Rev., 106, 1317-1331.

Newton, C. W., and J. C. Fankhauser, 1964: On the movements of convective storms with emphasis on size discrimination in relation to water budget requirements. J. Appl. Meteorol., 3, 651-668.

_____, 1966: Circulations in large sheared cumulus. Tellus, 18, 699-713.

Palmen, E., and E. O. Holopainen, 1962: Divergence, vertical velocity and kinetic energy in an extra-tropical disturbance. Geophysica, 8, 89-113.

Wilson, G. S., 1976: Large scale vertical motion calculations in the AVE-IV experiment. Geophys. Res. Lett., 3, 735-738.

Yanai, M., S. Esbensen, and J. Chu, 1973: Determination of bulk properties of tropical cloud clusters from large scale heat and moisture budgets. J. Atmos. Sci., 30, 611-627.